

Surface Life Challenges in Machine Elements

Guillermo E. Morales-Espejel

SKF Research and Technology Development
Houten, The Netherlands



Contents

1. A Changing World for Tribological Surfaces
2. Tribology Modelling of Emerging Failure Modes
3. New Concepts in the Life of Machine Elements

A Changing World for Tribological Surfaces

SKF A Changing World for Rolling Bearings



Max Pressure ~ 2-4 GPa (weight of 10 cars on a fingernail)

Load cycles ~ 1×10^{11} (no. stars in 1000 Galaxies)

Film Thickness ~ 100 nm (~ 2 piled up viruses)

Sliding ~ 0-5% (~ 4 m/s)



Max Pressure ~ 1-2 GPa (weight of 1.5 cars on a fingernail)

Load cycles ~ 1×10^8 (no. stars in 1 Galaxy)

Film Thickness ~ 300 nm (~ 6 piled up viruses)

Sliding ~ 0-30% (~ 20 m/s)

Industry Megatrends



Electrification

New lubricants, quiet, faster, hotter, more load, new failure modes

Energy Efficiency

Poorer lubrication, faster, hotter

Speed (Low and High)

Low: Poor lubrication, wear, surface fatigue

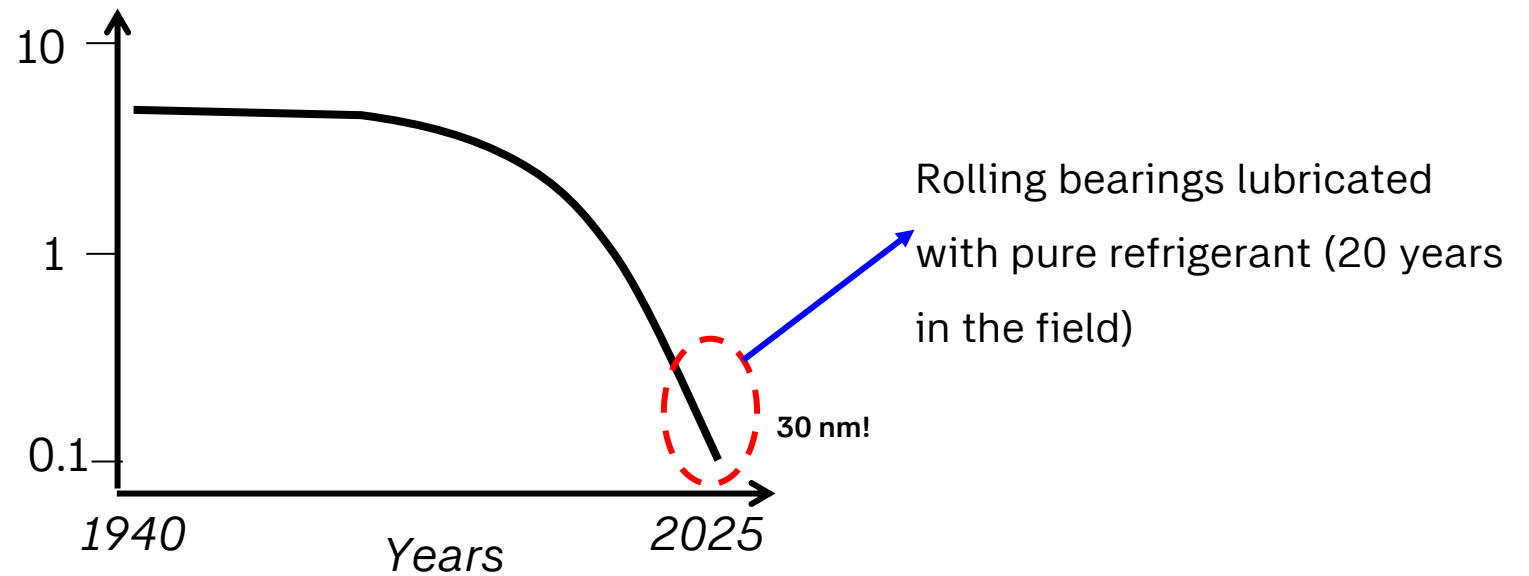
High: Starvation, adhesive wear

(*) Morales-Espejel, G.E., Surface Life Modelling of Tribological Components – From Surface Roughness to Bearings and Gear Life, Tribology Online, Vol. 18, No. 6 (2023) 255-267.

TRIBOLOGY TODAY, Istanbul Turkey, 13-17 April 2026

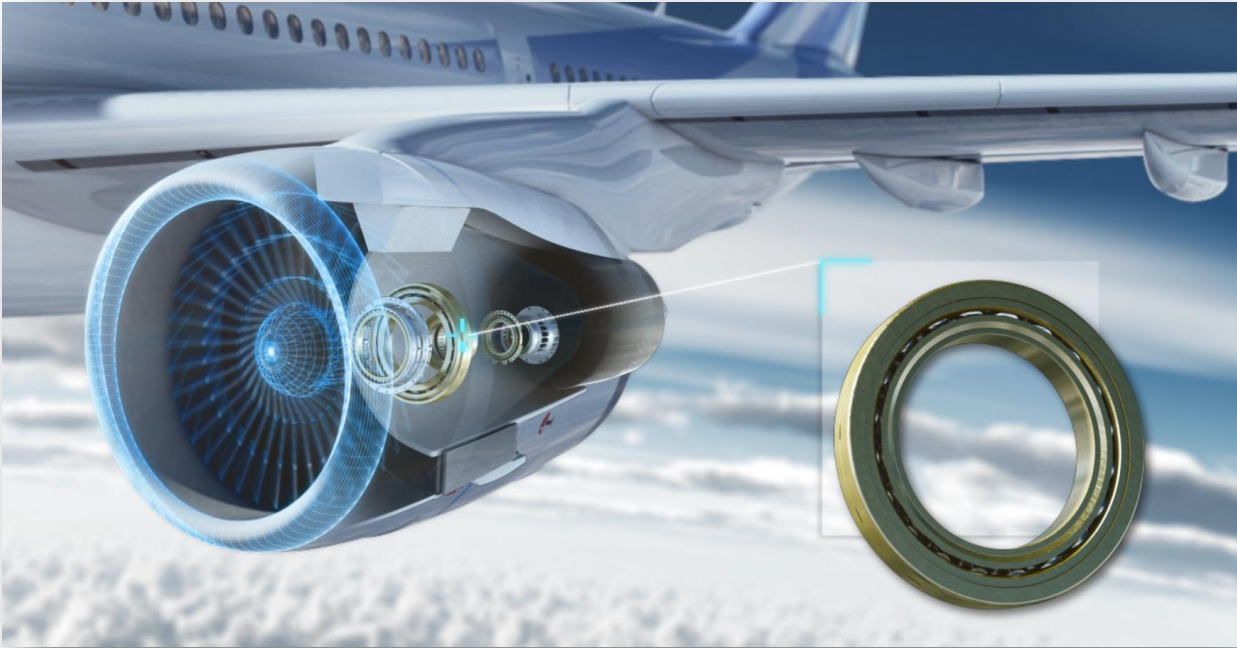
The Thinning Film Thickness in Rolling Bearings

Film Thickness (bearings) [μm]



Extending Dowson's Book*

Rolling Bearing Trends: Aero-Engines



Challenges:

- High temperatures ($\sim 300^{\circ}\text{C}$)
- High loads
- High speeds $ndm \sim 3 \times 10^6$

$n = \text{rpm}$

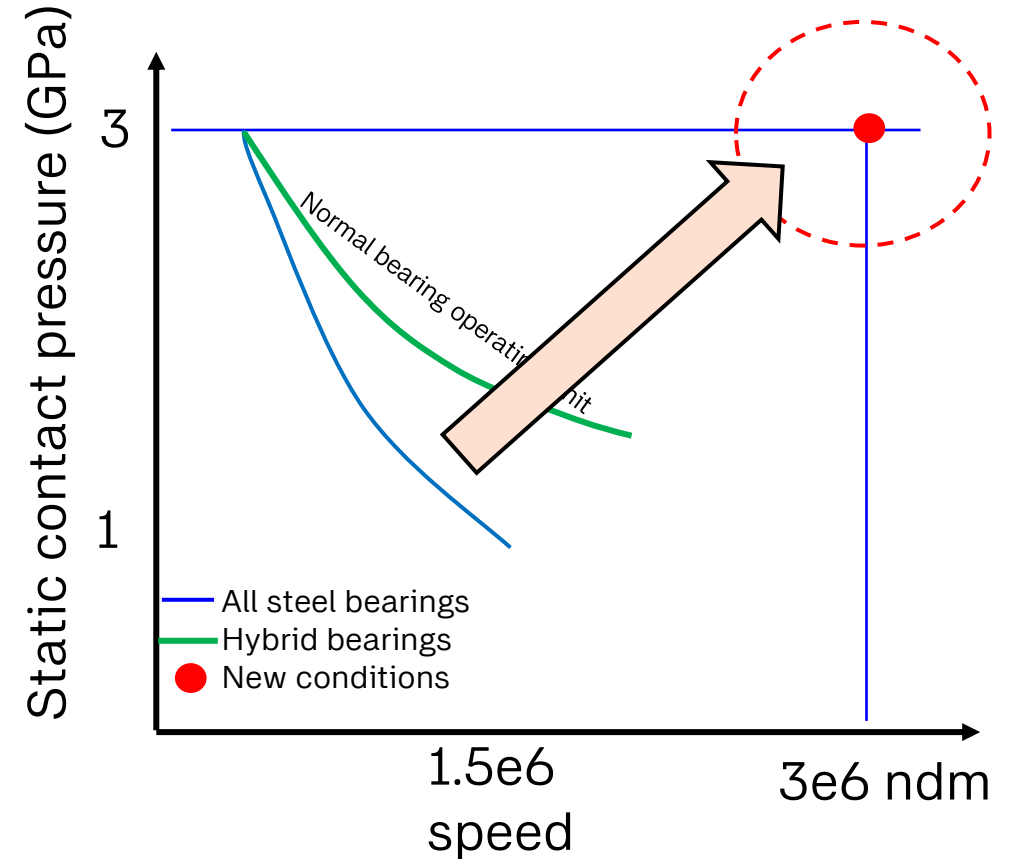
$dm = \text{bearing mean diameter in mm}$

Rolling Bearing Trends: Machine Tool Spindles

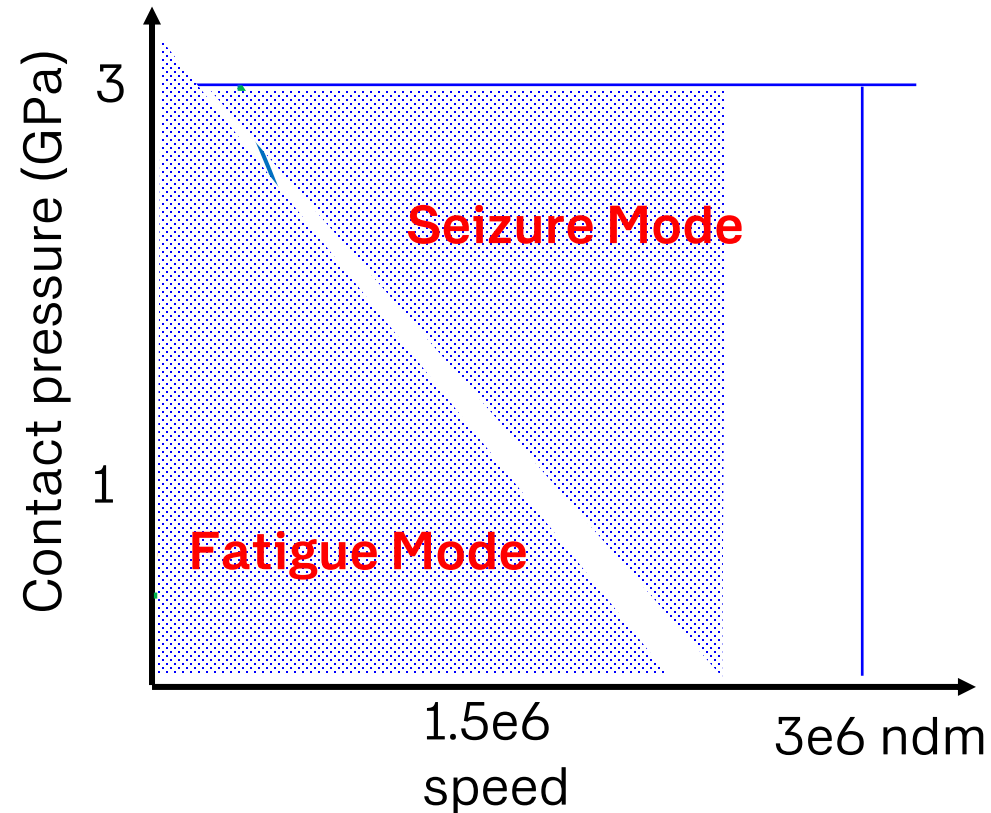


Challenges:

- Stiffness (accuracy)
- Cleanliness
- High speeds + High loads



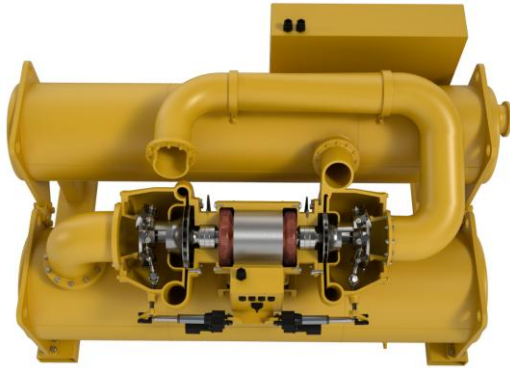
Competition of Fatigue with Frictional Heating



H. Czichos and K. Kirschke. Investigation into Film Failure (Transition Point) of Lubricated Concentrated Contacts. *Wear*, 22, pages 321–336, 1972.

Rolling Bearing Trends: Compressors and Pumps

Refrigeration Compressors



- Temperature: 30⁰C - 50⁰C
- Refrigerant dilution: <30 %
- Contact pressures: ~1.2 GPa
- Corrosive refrigerants



Industrial Heat Pumps

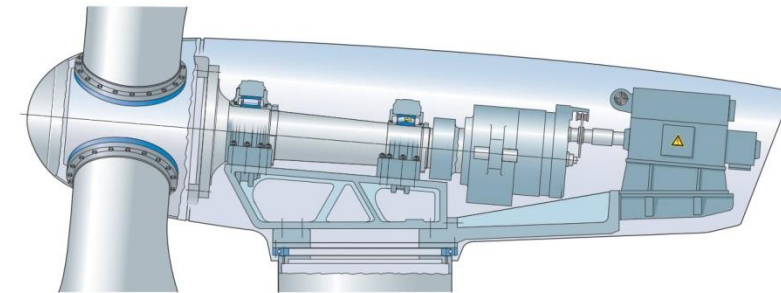
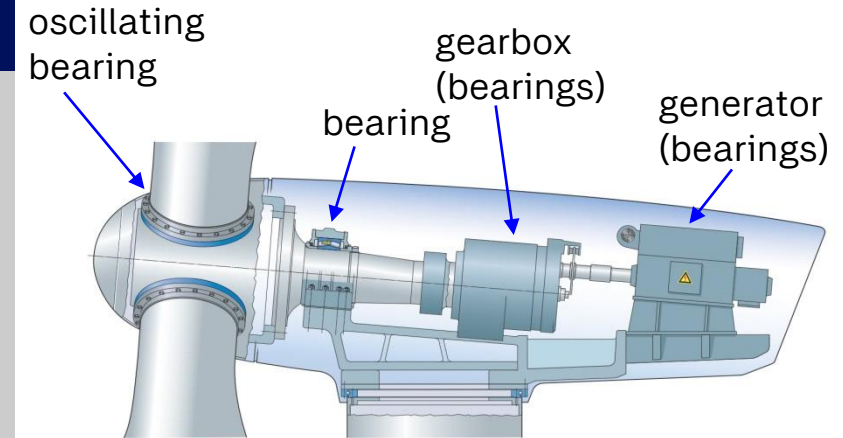
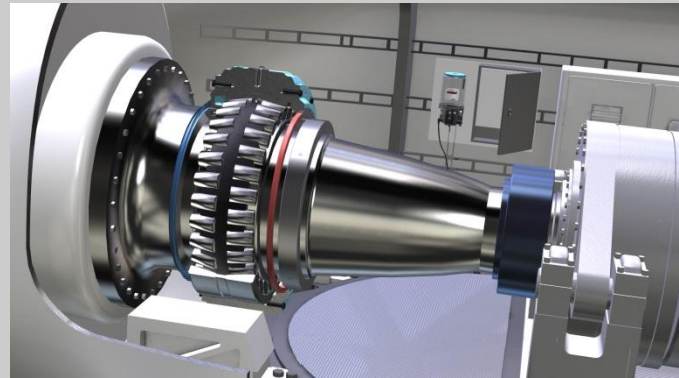


- Temperature: 100⁰C - 200⁰C
- Refrigerant dilution: <60 %
- Contact pressures: ~1.5 GPa
- More corrosive refrigerants

Rolling Bearing Trends: Wind Turbines



Wind turbine with gearbox



Challenges:

- For gearboxes: Dynamic loads, poor lubrication, particle contamination
- For main shaft: Structural stresses, fretting (creep), poor lubrication (grease)
- Slewing bearings: Wear, fretting

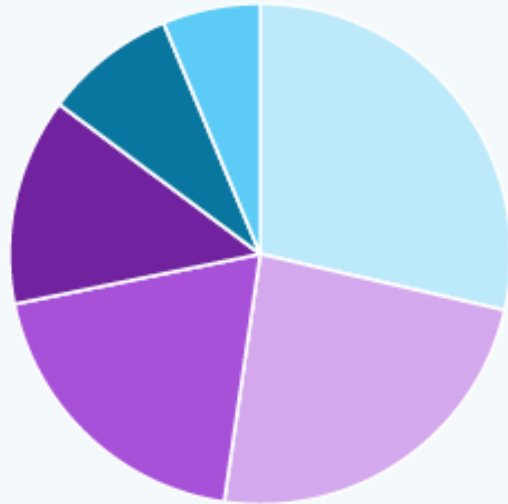
Electrification beyond Mobility



SKF Frequency Converters

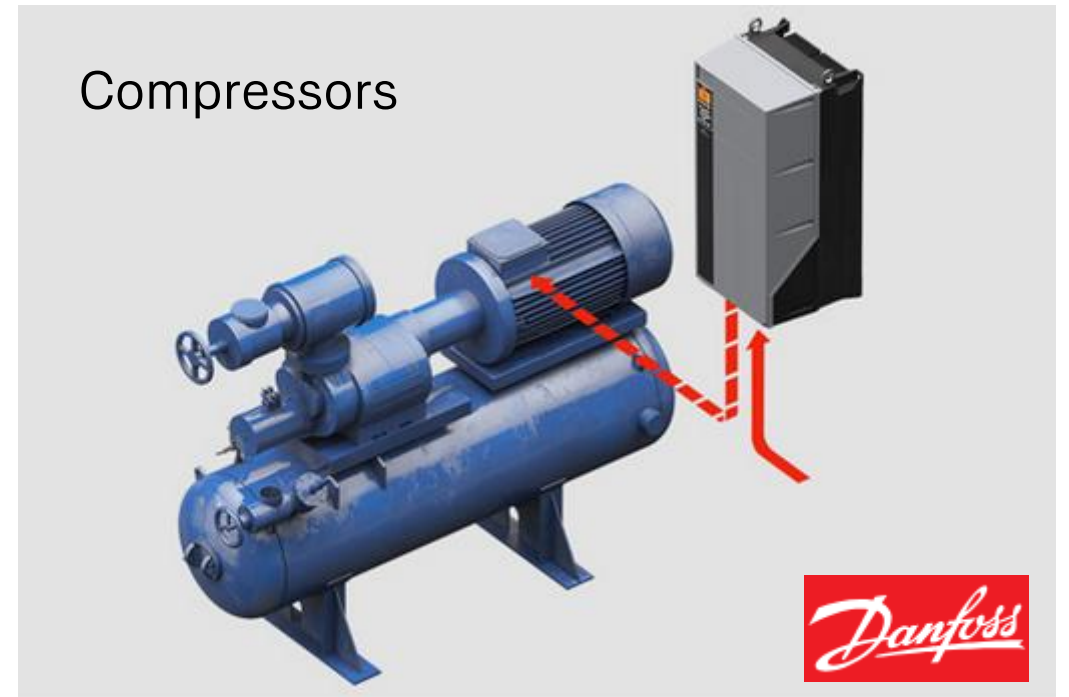
Frequency Converter Market Share

by End Use, 2023 (%)

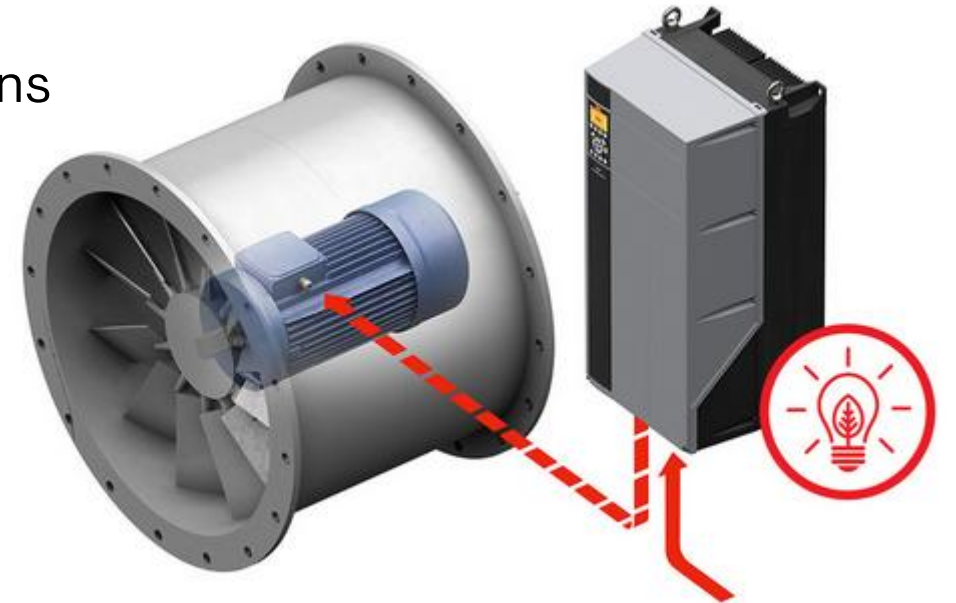


● Aerospace & Defense ● Power & Energy ● Process Industry ● Oil & Gas
● HVAC ● Others

HVAC = Heating, Ventilation and Air Conditioning



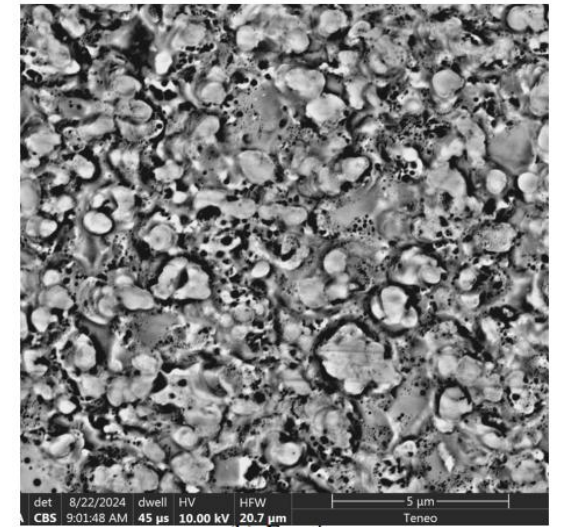
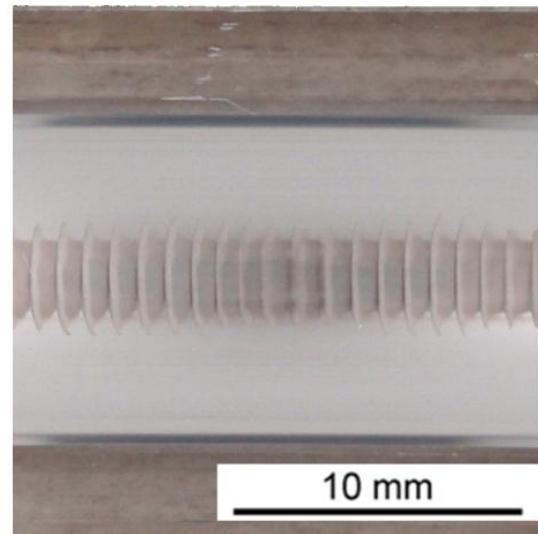
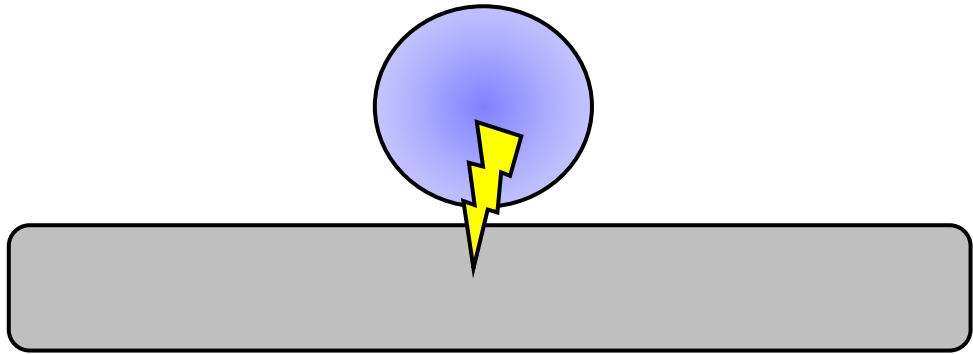
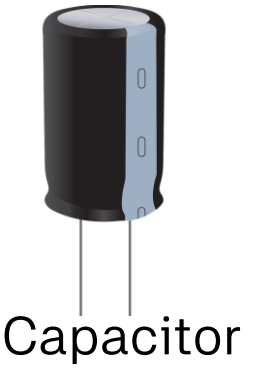
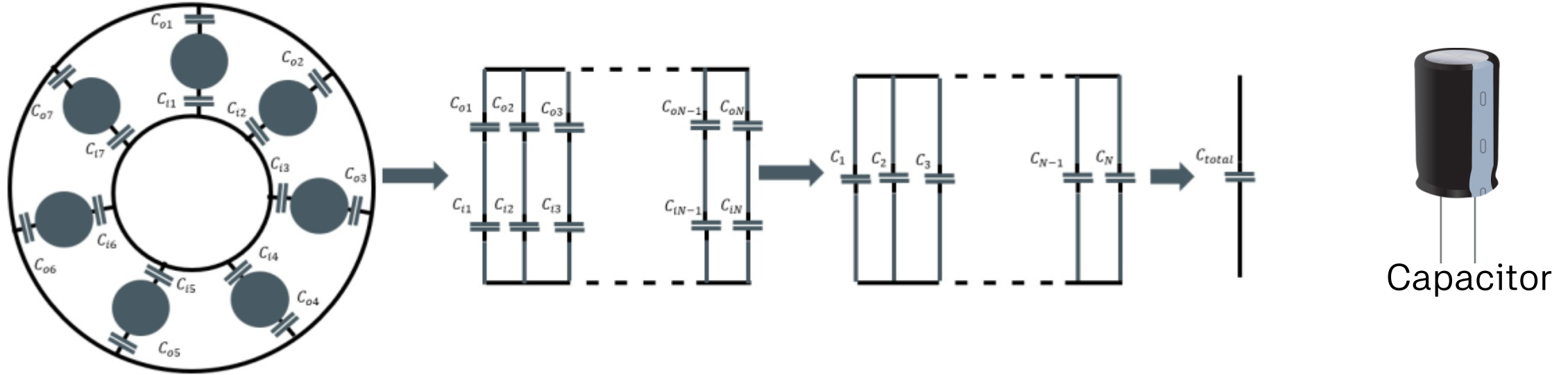
Fans



(*) Frequency Converter Market Size, Share & Trends Analysis Report By Type (Static, Rotary),
By Phase (Single Phase, Three Phase), By End Use, By Region, And Segment Forecasts, 2024 – 2030
Grand View Report ID: GVR-4-68040-387-5

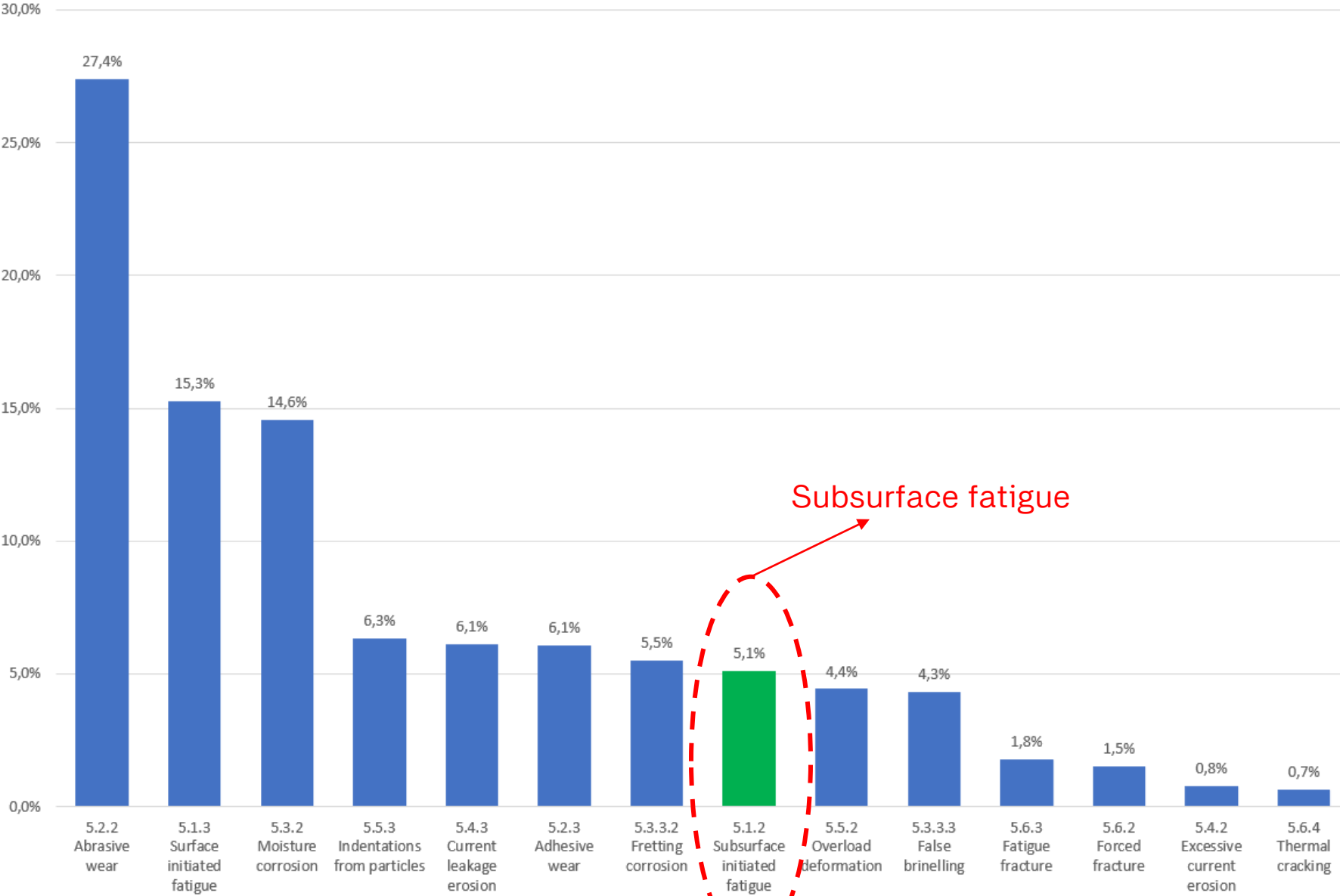
TRIBOLOGY TODAY, Istanbul Turkey, 13-17 April 2026

Electrical Damage in Bearings



Tribology Modelling of Emerging Failure Modes

SKF Modern Failure Statistics in Bearings



Source: SKF field failure statistics

Lubrication

SKF Numerical Solution of EHL

Classical Solution Methods:

- Multigrid (Lubrecht and Venner)
- FEM Full System (Habchi et al.)
- Others

- Reynolds Equation:

$$\underbrace{\frac{\partial}{\partial x} \left(\frac{\rho h^3}{\eta} \frac{\partial p}{\partial x} \right) + \frac{\partial}{\partial y} \left(\frac{\rho h^3}{\eta} \frac{\partial p}{\partial y} \right)}_{\text{Poiseuille flow}} = \underbrace{12\bar{u} \frac{\partial(\rho h)}{\partial x}}_{\text{Couette flow}} + \underbrace{12 \frac{\partial(\rho h)}{\partial t}}_{\text{squeeze film term}}$$

- Film Thickness Equation:

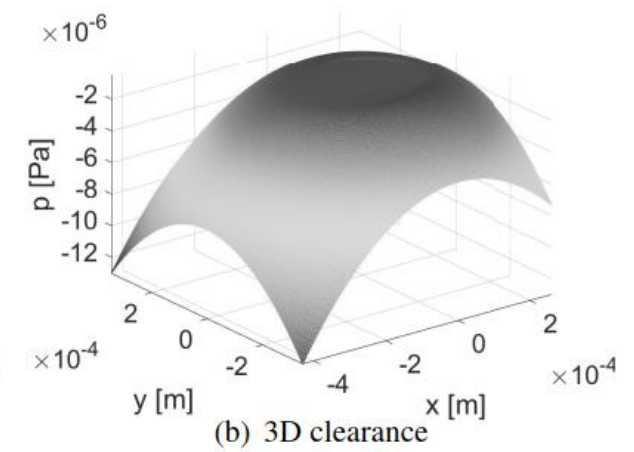
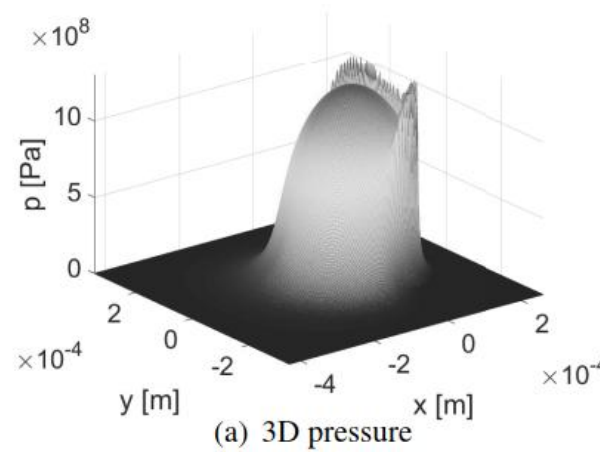
$$h(x,y) = \underbrace{h_0}_{\text{constant approach}} + \underbrace{\frac{x^2}{2R_x} + \frac{y^2}{2R_y}}_{\text{parabolic}} + \underbrace{\frac{2}{\pi E'} \int_{-\infty}^{\infty} \int_{-\infty}^{\infty} \frac{p(x',y')}{\sqrt{(x-x')^2 + (y-y')^2}}}_{\text{elastic deformation}}$$

- Load Equilibrium Equation:

$$Q = \int_{-\infty}^{\infty} \int_{-\infty}^{\infty} p(x,y) dx dy$$

- State Equation for Lubricant

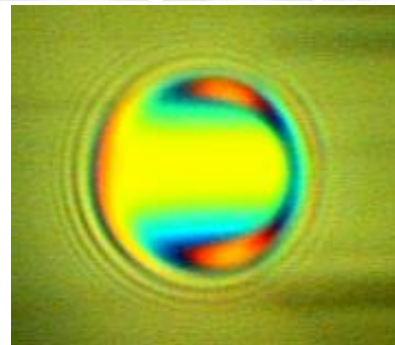
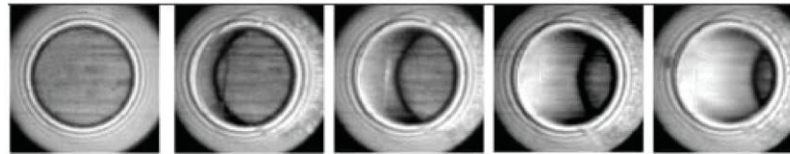
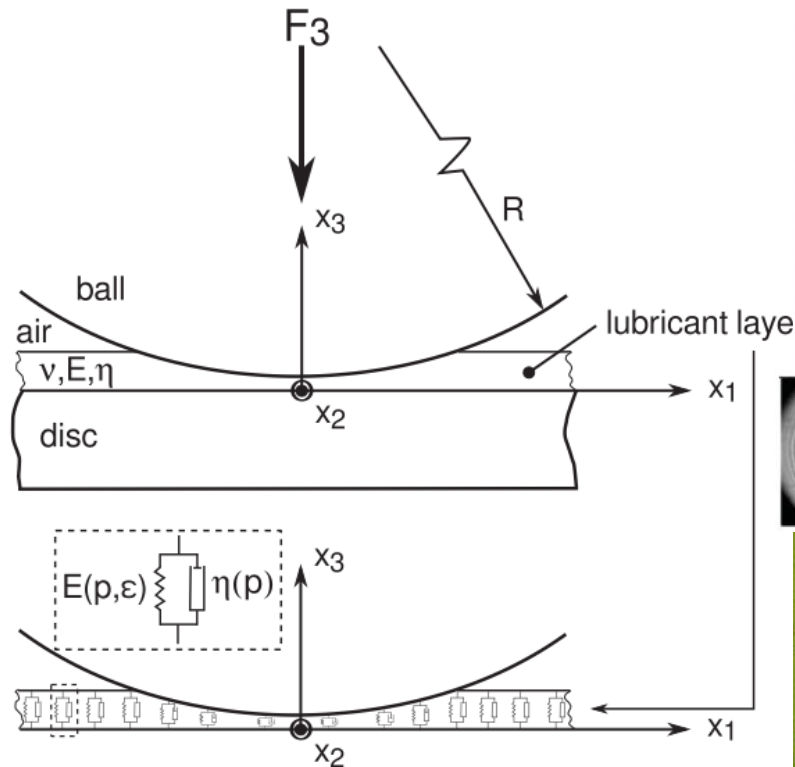
$$\rho(p) = f_{\rho}(p) \quad \eta(p) = f_{\eta}(p)$$



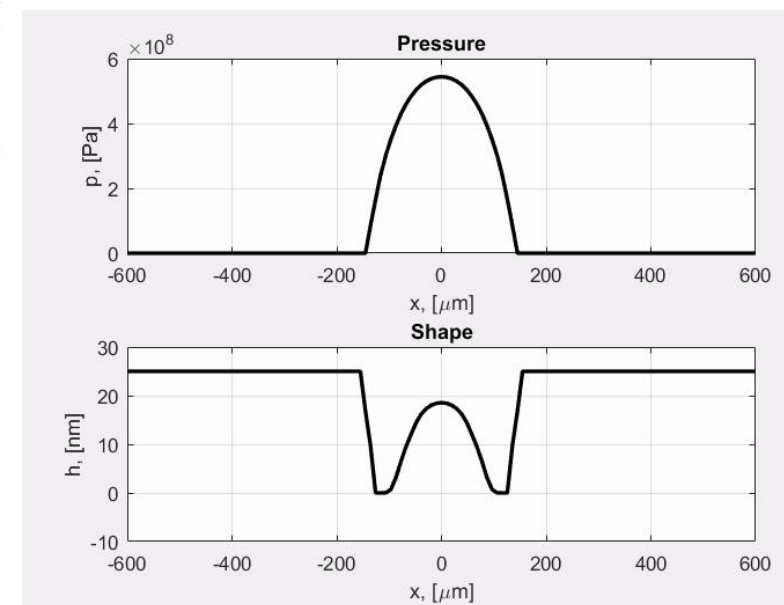
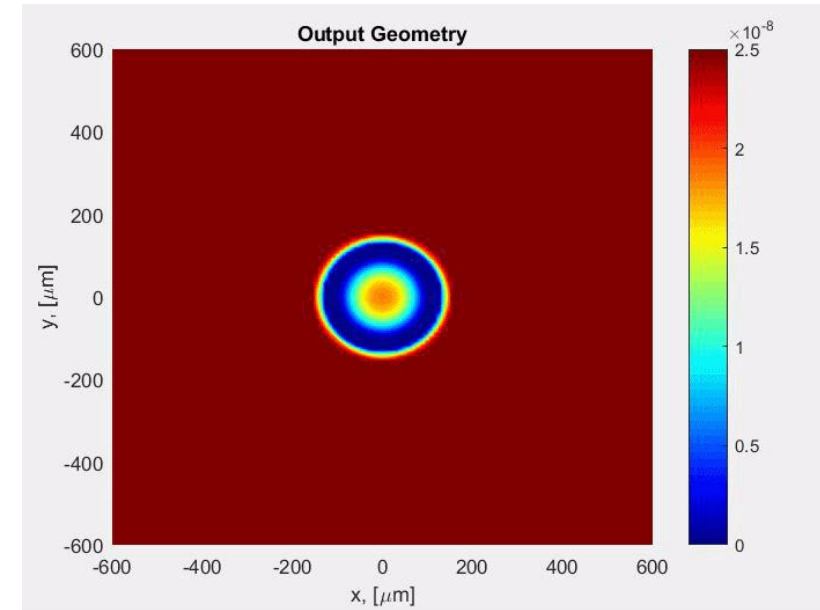
$$G = \alpha E', \quad W = \frac{Q}{(E' R_x^2)}, \quad U = \frac{\bar{u} \eta_0}{E' R_x}, \quad H_D = h/R_x, \quad P_D = p/E'$$

SKF Exploring New Ways of Modelling Lubrication

Towards proper modelling of “mixed-Lubrication”



Glovnea & Spikes



* van Emden, E., Venner, C.H., Morales-Espejel, G.E., “Investigation into the viscoelastic behaviour of a thin lubricant layer in an EHL contact”, Trib. Inter., vol. 111, pp. 197-210, 2017

* Glovnea, R. P., Spikes, H. A., “Elastohydrodynamic film formation at the start-up of the motion”, Proc. IMechE, part J, vol. 215, pp. 125-138, 2001

SKF Inlet Analysis (Ertel-Grubin) - A Reminder

Consider the line contact steady-state Reynolds equation:

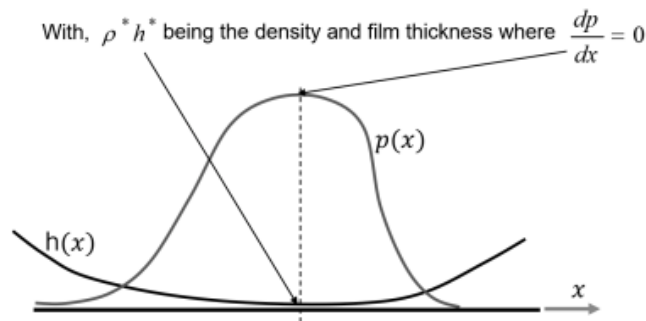
$$\frac{\partial}{\partial x} \left(\frac{\rho h^3}{12\eta} \frac{\partial p}{\partial x} \right) = \bar{u} \frac{\partial(\rho h)}{\partial x}$$

Therefore, integrating one time in x :

$$\int_0^{\rho h} \left(\frac{\rho h^3}{12\eta} \frac{\partial p}{\partial x} \right) \partial \left(\frac{\rho h^3}{12\eta} \frac{\partial p}{\partial x} \right) = \bar{u} \int_{\rho^* h^*}^{\rho h} \frac{\partial(\rho h)}{\partial x} \partial x$$

$$\frac{dp}{dx} = 12\eta \bar{u} \frac{\rho h - \rho^* h^*}{\rho h^3}$$

with ρ^* and h^* being the values of density and film thickness where $dp/dx = 0$



Barus law: $\eta(p) = \eta_0 \exp(\alpha p)$

introduced, named “reduced pressure”, \hat{q} :

$$\hat{q} = [1 - \exp(-\alpha p)]/\alpha$$

which is now substituted

$$\frac{d\hat{q}}{dx} = 12\eta_0 \bar{u} \frac{\rho h - \rho^* h^*}{\rho h^3}$$

Introducing dimensionless groups:

$$X = x/a, \quad P = p/p_0, \quad \hat{H} = 2R_x h/a^2, \quad \hat{Q} = \hat{q}/\hat{q}_0, \quad K = \frac{48\bar{u}\eta_0 R_x^2}{a^3 p_0}$$

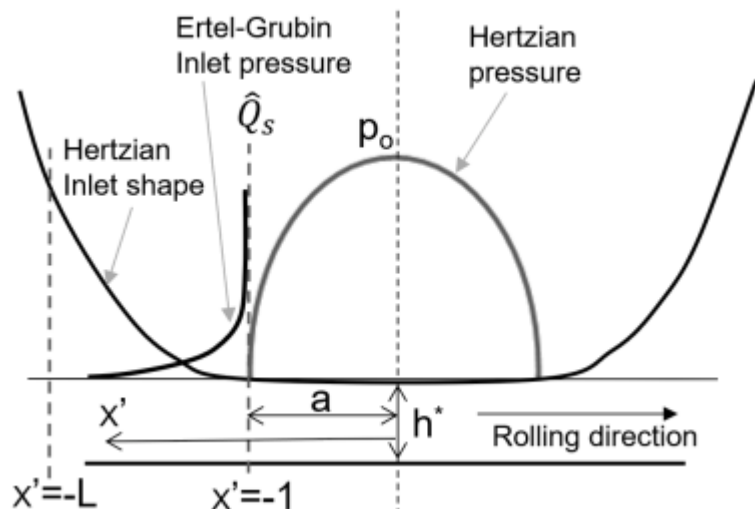
Notice that the dimensionless pressures can be recovered from $P = -\frac{1}{K_1} \ln(1 - K_1 \hat{Q})$, with $K_1 = \alpha p_0$.

The Reynolds equation can be rewritten:

$$\frac{d\hat{Q}}{dX} = K \frac{\hat{H} - \hat{H}^*}{\hat{H}^3}$$

Integrating

SKF Inlet Analysis (Ertel-Grubin) - A Reminder



at the end of the inlet (where $x' = -a$) the pressure is so high that can be assumed as $\hat{Q} = \hat{Q}_s = 1/K_1$ at $X' = -1$

$$\int_{\hat{Q}_s}^{\hat{Q}} d\hat{Q} = -K \int_{X'=-1}^{X'} \frac{\hat{H} - \hat{H}^*}{\hat{H}^3} dX'$$

$$\hat{Q} = \hat{Q}_s - K \int_{X'=-1}^{X'} \frac{\hat{H} - \hat{H}^*}{\hat{H}^3} dX'$$

Then,

$$\hat{Q} = \frac{1}{K_1} - K \int_{X'=-1}^{X'} \frac{\hat{H} - \hat{H}^*}{\hat{H}^3} dX'$$

Finally, applying the second set of boundary conditions, at $X' = -L$ being $L \approx \infty$ then $P = \hat{Q} = 0$. Then,

$$0 = \frac{1}{K_1} - K \int_{X'=-1}^{-L} \frac{\hat{H} - \hat{H}^*}{\hat{H}^3} dX'$$

Introducing the shape of the deformed surface outside the Hertz flat zone:

$$\hat{H} - \hat{H}^* = |X|(X^2 - 1)^{1/2} - \ln \left[|X| + (X^2 - 1)^{1/2} \right]$$

The above Reynolds equation can be solved iteratively for \hat{H}^* .

With this solution, Ertel-Grubin obtained a curve-fitted equation in

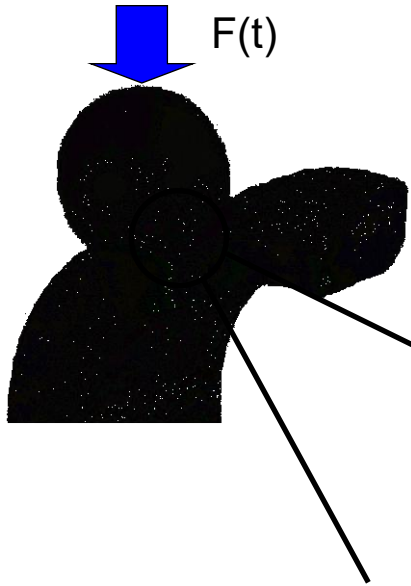
Terms of Dowson-Higginson parameters:

$$H_D^* = 1.95(GU)^{8/11} W^{-1/11} \approx 1.95(GU)^{0.73} W^{-0.091}$$

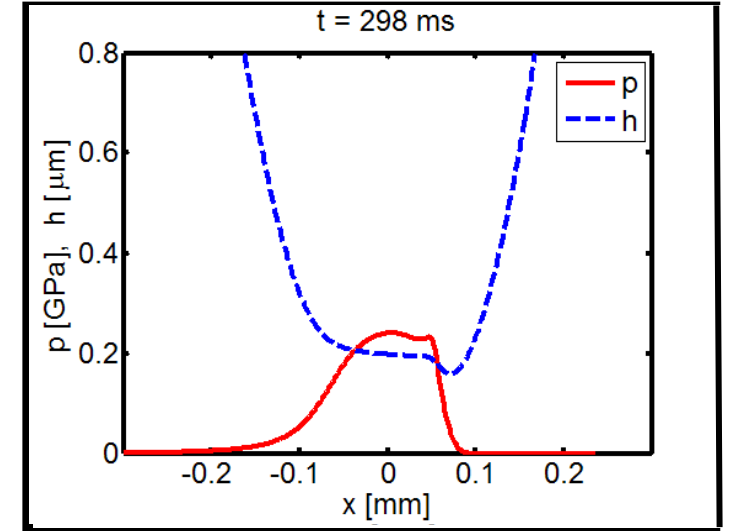
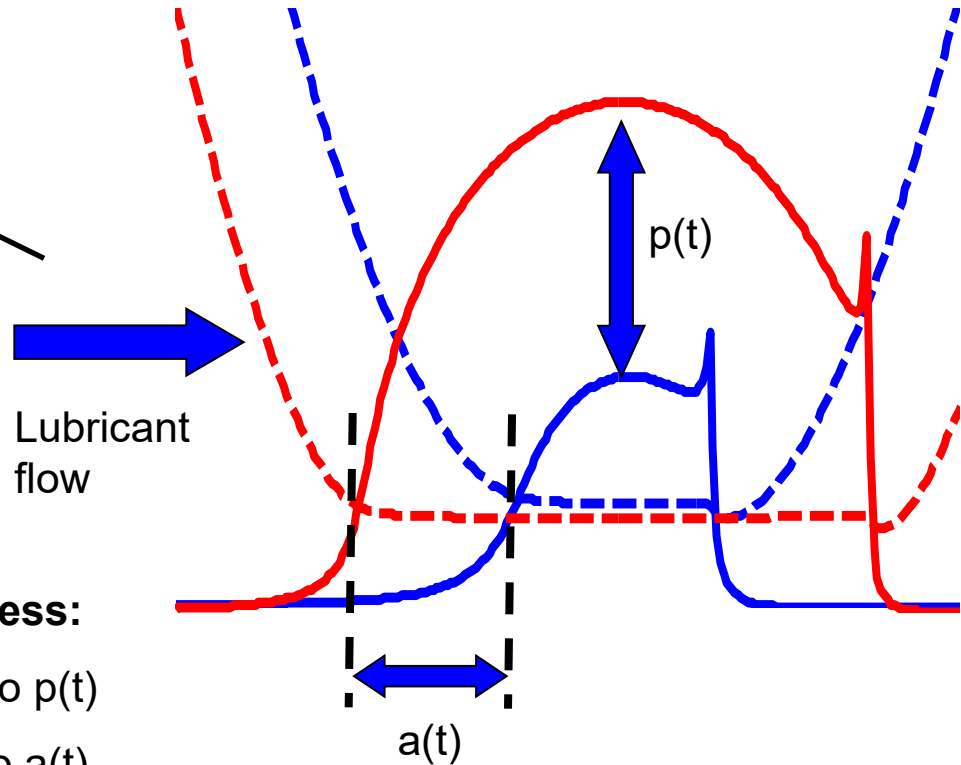
The inlet pressure can be recovered with:

$$P = -\frac{1}{K_1} \ln(1 - K_1 \hat{Q})$$

SKF Dynamic Effects in Lubrication – The Inlet



Typical EHL pressure and film thickness profiles



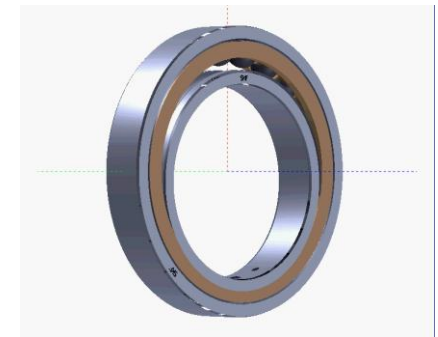
Numerical Simulation with Sinusoidal Normal Load

Effects on the film thickness:

- Global film squeeze due to $p(t)$
- Inlet film fluctuation due to $a(t)$,
i.e. $u = u_0 + da/dt$

1. Morales-Espejel, G.E., "Central film thickness in time-varying normal approach of rolling elastohydrodynamically lubricated contacts", IMechE, part C vol. 222, pp. 1271-1280, 2008

2. Félix-Quiñonez, A., Morales-Espejel, G.E., "Film thickness in time-varying normal loading of rolling elastohydrodynamically lubricated contacts", IMechE, part C vol. 224, pp. 2559-2567, 2010



SKF Transient Ertel-Grubin Model

The Reynolds equation 1D, transient is:

$$\frac{\partial}{\partial x} \left(\frac{\rho h^3}{\eta} \frac{\partial p}{\partial x} \right) = 12\bar{u} \frac{\partial(\rho h)}{\partial x} + 12 \frac{\partial(\rho h)}{\partial t}$$

Corrected to consider variation of contact semi-width in time

The first integration respect to x gives:

$$\frac{\partial p}{\partial x} = 12\bar{u}\eta \frac{\rho h - \rho^* h^*}{\rho h^3} + \frac{12\eta}{\rho h^3} \int_{x^*}^x \frac{\partial(\rho h)}{\partial t} dx$$

Introducing dimensionless groups, gives:

$$X = \frac{x}{a}, \quad \hat{H} = \frac{2R_x h}{a^2}, \quad P = \frac{p}{p_o}$$

$$Q = \frac{q}{p_o}, \quad K = \frac{48\bar{u}\eta_o R_x^2}{(a^3 p_o)} \quad K_1 = \alpha p_o$$

$$\hat{T} = t\bar{u}/a \quad q = [1 - e^{-\alpha p}]/\alpha$$

$$\frac{\partial Q}{\partial X} = \frac{K}{\hat{H}^3} \left(\hat{H} - \hat{H}^* + \int_{X=1}^X \frac{\partial \hat{H}}{\partial \hat{T}} dX \right)$$

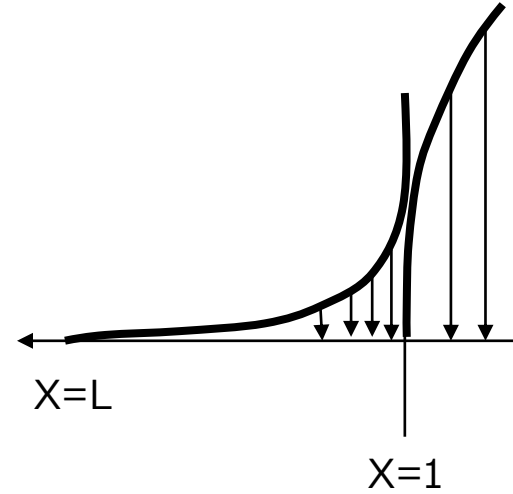
Applying Grubin boundary conditions for $X=1$, $Q=1/K_1$ and integrating, then applying $X=L \approx \infty$, $Q=0$

$$\frac{1}{K_r} = \int_{X=1}^L \frac{\hat{H}' - \hat{H}'^* + (d\hat{H}^*/d\hat{T})(X-1)}{\hat{H}'^3} dX$$

$$K_1 K = K_r = (48\bar{u}\eta_o R_x^2 \alpha) / (a^3)$$

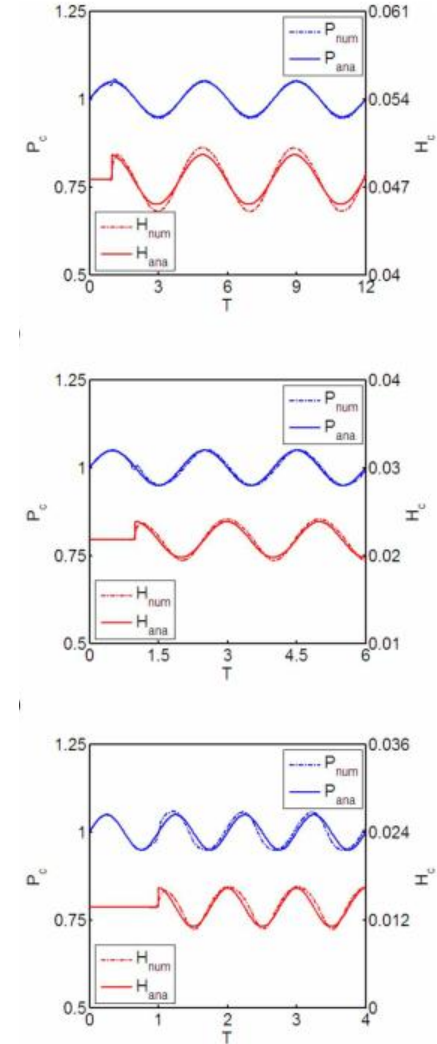
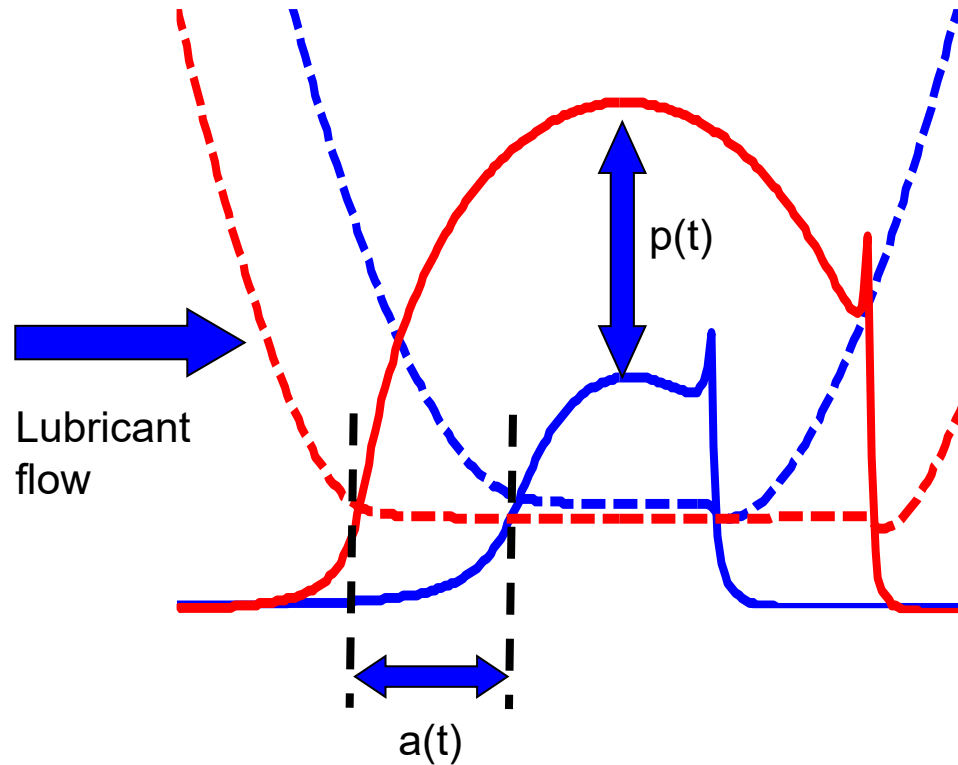
$$\text{Crook: } \hat{H}(X) = C(X-1)^{3/2} \quad ; C = \frac{4}{3}\sqrt{2}$$

$$\frac{\partial \hat{H}^*}{\partial \hat{T}} = \frac{C^{4/3} (\hat{H}^*)^{5/3}}{0.2687} \left[\frac{1}{K_r} - \frac{0.2687}{C^{2/3} (\hat{H}^*)^{4/3}} \right]$$



SKF Model Comparison

Typical EHL pressure and film thickness profiles

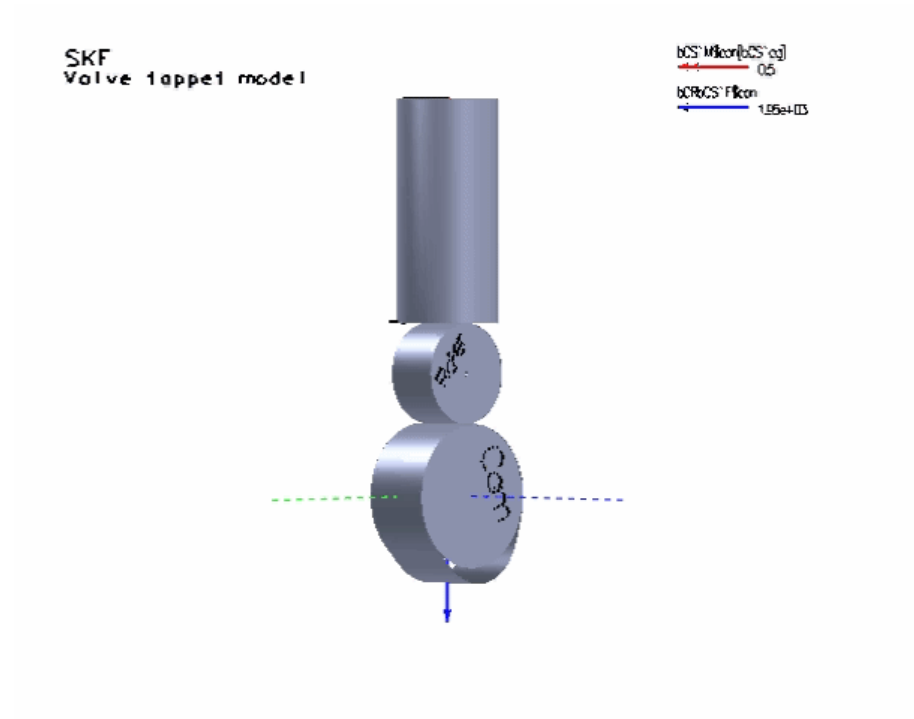
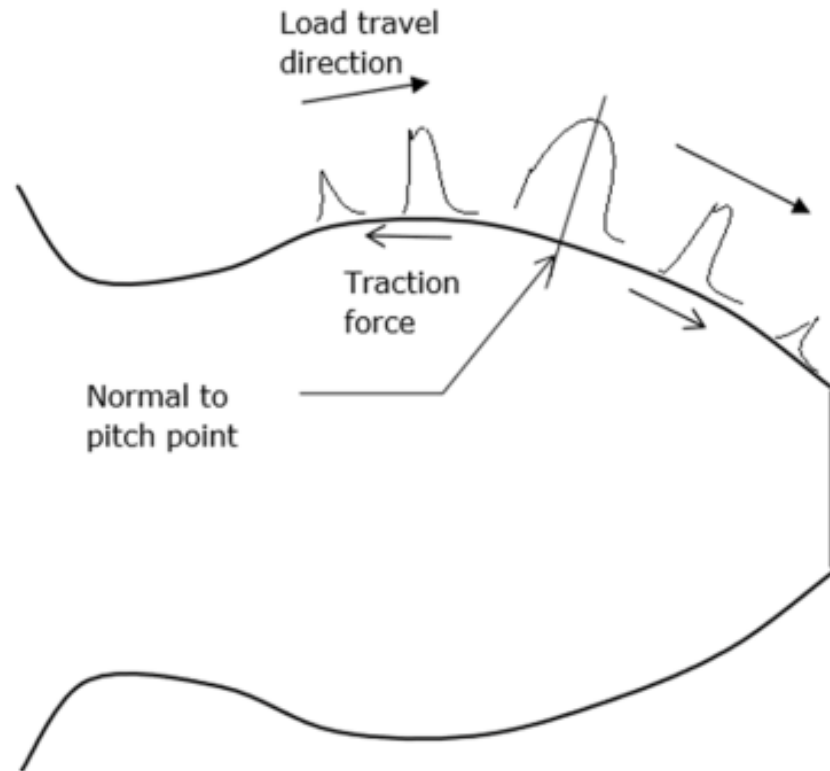


(c)

Comparison of numerical and analytical central film thickness and pressures as a function of time. The analytical results on the left-hand side figures correspond to the original method. The results including the proposed entrainment speed correction are given on the right-hand side plots: (a) $M = 40$, $L = 10$, $\Omega = 0.5\pi$, $A_w = 0.1$; (b) $M = 80$, $L = 10$, $\Omega = \pi$, $A_w = 0.1$; and (c) $M = 120$, $L = 10$, $\Omega = 2\pi$, $A_w = 0.1$

Félix-Quiñonez, A., Morales-Espejel, G.E., "Film thickness in time-varying normal loading of rolling elastohydrodynamically lubricated contacts", IMechE, part C vol. 224, pp. 2559-2567, 2010

Variable Speed



SKF Variable Speed

$$\frac{\partial}{\partial x} \left(\frac{\rho h^3}{\eta} \frac{\partial p}{\partial x} \right) = 12\bar{u} \frac{\partial(\rho h)}{\partial x} + 12 \frac{\partial(\rho h)}{\partial t} \quad \longrightarrow \quad \frac{\partial Q}{\partial X} = \frac{K}{\hat{H}^3} \left(\hat{H}' - \hat{H}^{*} + \frac{K_2}{\Delta \hat{T}} \int_{X=1}^X (\hat{H}' - \hat{H}) dX \right)$$

With H' for the dimensionless clearance for the time $t + \Delta t$ and H at time t

The term $(\hat{H}' - \hat{H})$ is independent of X , thus the final equation to solve is:

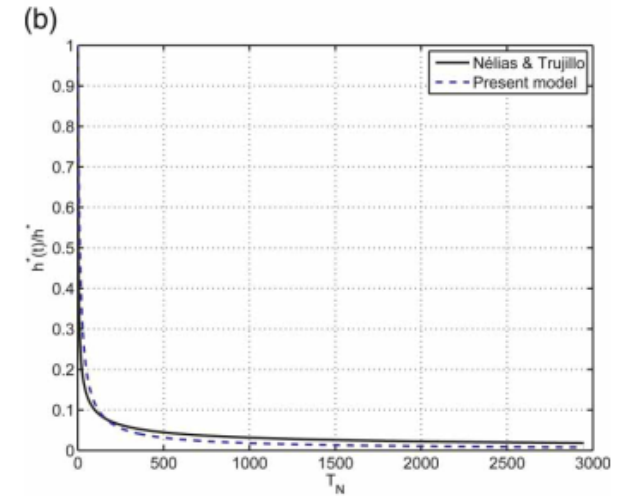
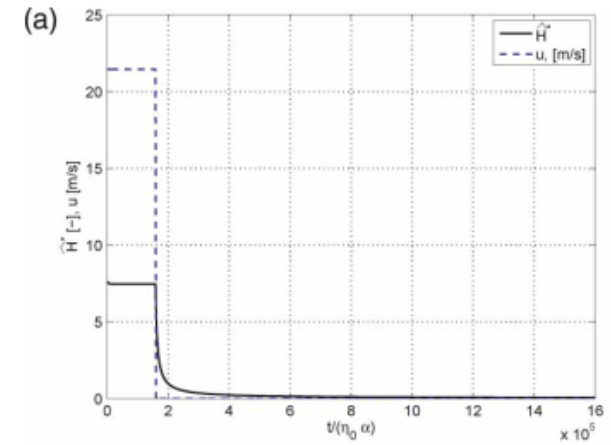
$$\frac{\partial Q}{\partial X} = \frac{K}{\hat{H}^3} \left(\hat{H}' - \hat{H}^{*} + K_2 \frac{\hat{H}' - \hat{H}}{\Delta \hat{T}} (X - 1) \right)$$

With:

$$\tilde{T} = t / (\eta_0 \alpha). \quad K_2 = a / \eta_0 \bar{u} \alpha$$

Table 1 Steady-state data used in the sudden halting example

F (N)	α (GPa) ⁻¹	E' (GPa)	η_0 (Pa s)	R_x (m)	\bar{u} (m/s)	p_0 (GPa)	K (-)	K_1 (-)	K_2 (-)	H^* (-)
1022	22.81	226	0.4247	0.0087	21.45	1.17	5.0	26.67	854.8	7.63

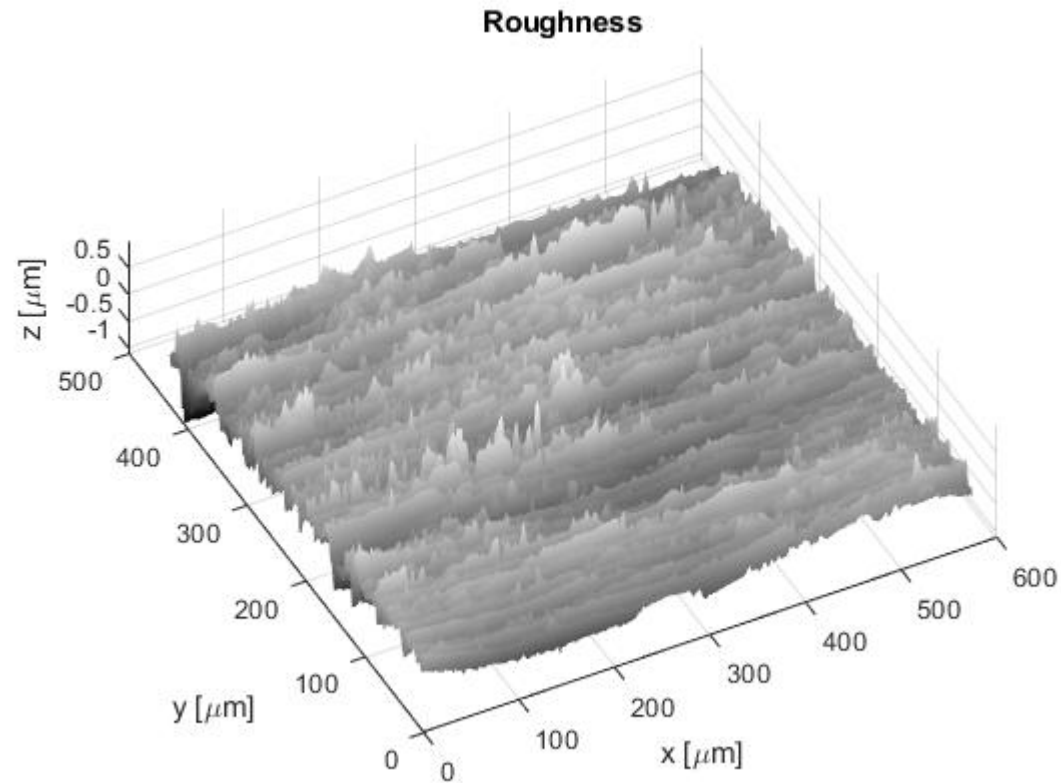


- 1** Sudden halting motion for example 1 of Table 1, initial values $K = 5.0$, $K_1 = 26.67$, and $K_2 = 854.8$. (a) variation of \bar{u} and \hat{H}_c in time, \hat{I} and (b) comparison with model of reference [17]

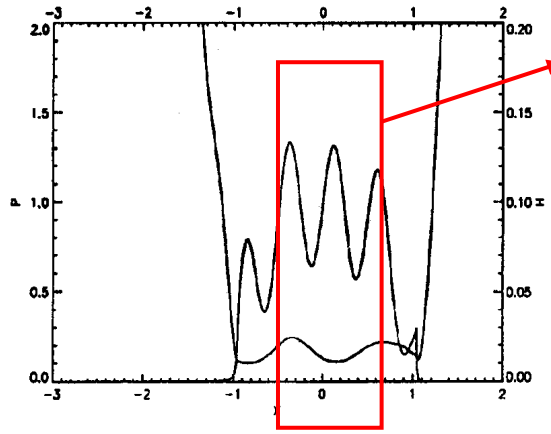
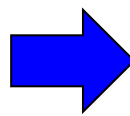
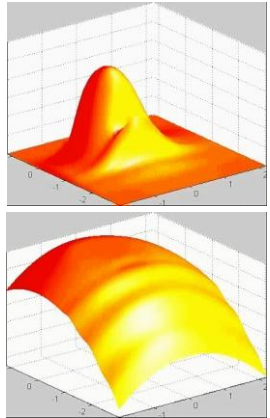
Morales-Espejel, G.E., Wemekamp, A.W. "Ertel-Grubin Methods in Elastohydrodynamic Lubrication – A Review", IMechE, part J vol. 222, pp. 15-34, 2008

* Nélías, D., Trujillo Jiménez, A., "A Simplified Model to Study EHL Film Collapse During Rapid Halting Motion. Tribol. Trans., 2002, 45(4), 512–520.

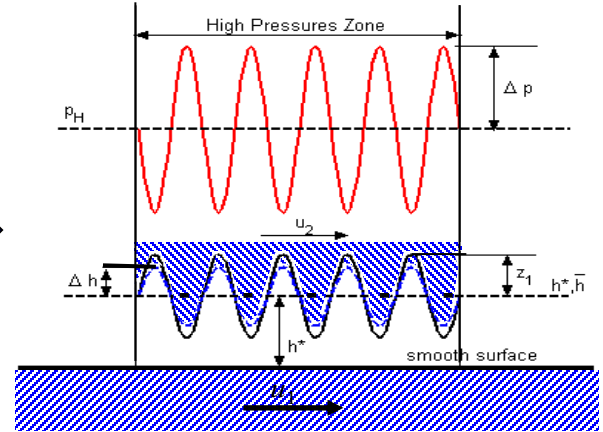
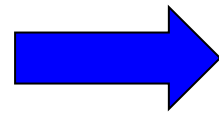
Modelling EHL with Roughness (Deterministic)



SKF Rapid Methods for Micro-EHL



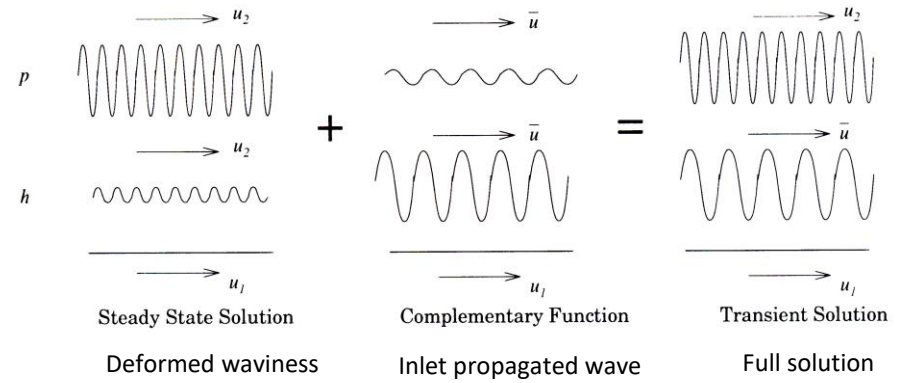
Central Zone



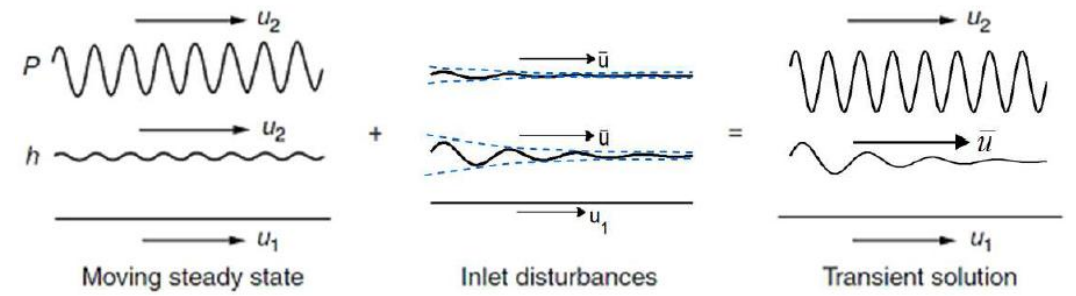
$$\frac{\partial}{\partial x} \left(\frac{\rho h^3}{12\eta} \frac{\partial p}{\partial x} \right) = \bar{u} \frac{\partial \rho h}{\partial x} + \frac{\partial \rho h}{\partial t}$$

- Linearised Reynolds Equation
- Use powerful Fourier techniques

Newtonian Behaviour



Non-Newtonian Behaviour



* Greenwood, J.A., Morales-Espejel, G.E., "The Behaviour of Transverse Roughness in EHL Contacts", IMechE, part J, vol. 208, pp. 121-132, 1994

* Hooke, C.J., Li, K.Y., Morales-Espejel, G.E., "Rapid calculation of the pressures and clearances in Rough rolling-sliding elastohydrodynamically lubricated contacts. Part1: Low-amplitude sinusoidal roughness", IMechE, part J, vol. 224, pp. 621-637, 2010

SKF Newtonian Model

- Steady State Solution: Steady state solution for pure sliding

$$h = \bar{h} + z + v \quad h(x) = \bar{h} + h_1 \sin\left(\frac{2\pi x}{\lambda}\right) \quad z(x) = z_1 \sin\left(\frac{2\pi x}{\lambda}\right) \quad p(x) = p_o + p_1 \sin\left(\frac{2\pi x}{\lambda}\right) \quad v(x) = v_1 \sin\left(\frac{2\pi x}{\lambda}\right)$$

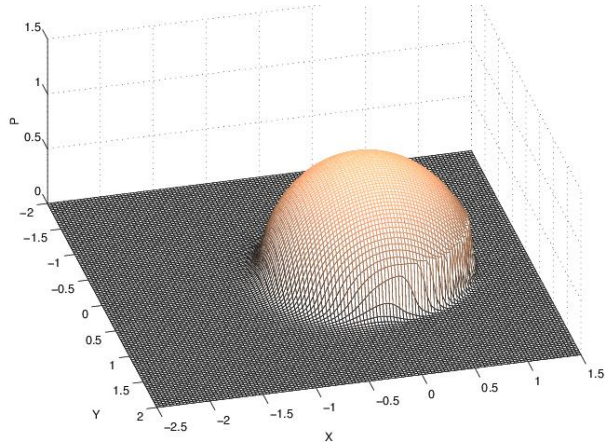
$$v_1 = \frac{2\lambda p_1}{\pi E'} \quad \rho h = \bar{\rho} \bar{h} \quad \text{with} \quad \frac{\rho(p)}{\rho(p_H)} \approx 1 + C(p - p_H) / \bar{h} \quad \text{from which:}$$

$$p_1 = \frac{-z_1}{C + A}, \quad h_1 = \frac{z_1 C}{C + A} \quad A = \frac{2\lambda}{\pi E'} \quad C = \frac{(\gamma - \beta) \bar{h}}{(1 + \gamma p_H)(1 + \beta p_H)}$$

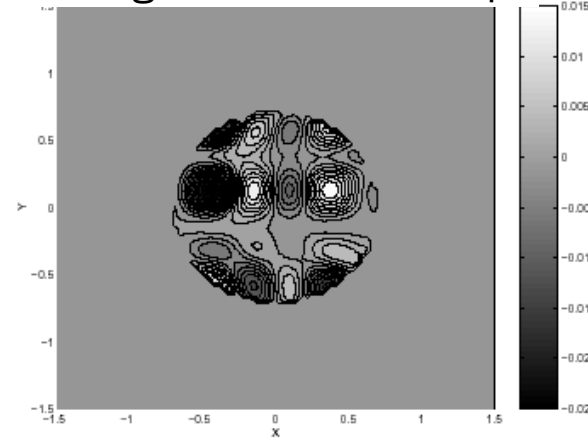
- Complementary Function: Inlet excitation from a partly deformed roughness

$$\frac{\partial}{\partial x} \left(\frac{\rho h^3}{12\eta} \frac{\partial p}{\partial x} \right) = \bar{u} \frac{\partial \rho h}{\partial x} + \frac{\partial \rho h}{\partial t} \quad \bar{u} \frac{\partial r}{\partial x} + \frac{\partial r}{\partial t} = 0 \quad r = \frac{\rho h}{\bar{\rho} \bar{h}} \quad (\text{oil flow})$$

SKF Comparison with Numerical Models

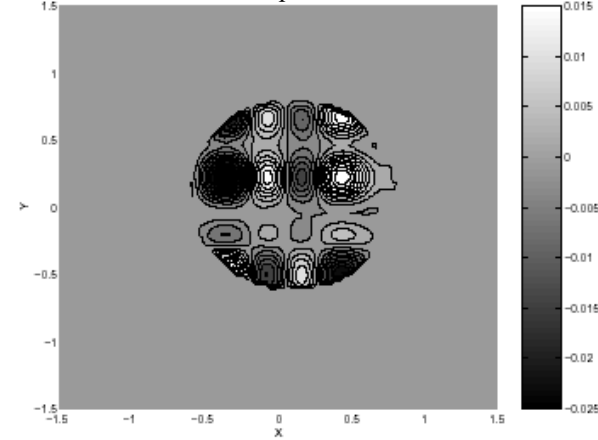


Multigrid Deformed Shape

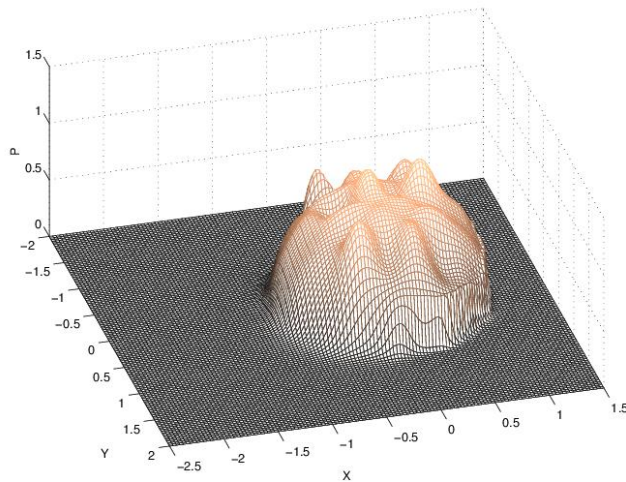


(a) Deformed roughness, numerical solution

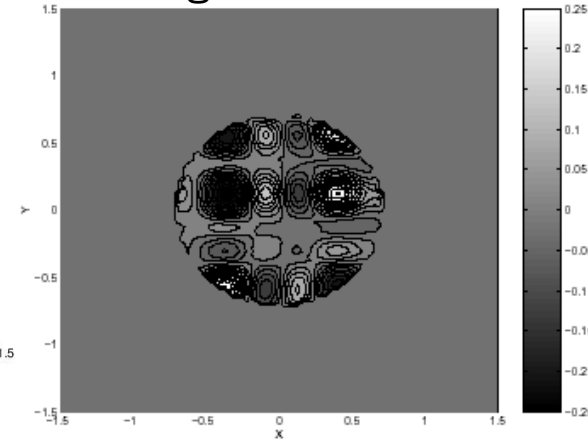
Rapid Method Deformed Shape



(b) Deformed roughness, present scheme

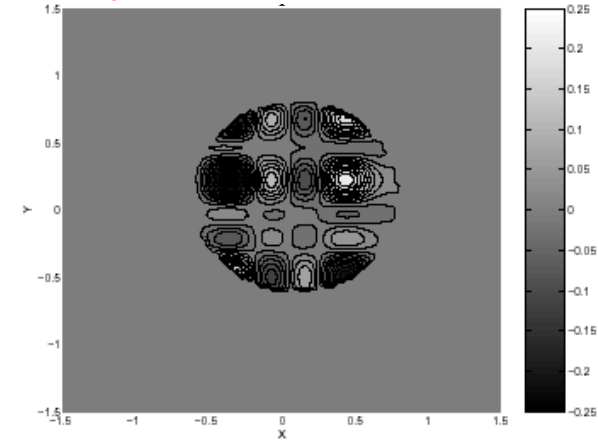


Multigrid Pressures



(c) Pressure ripples, numerical solution

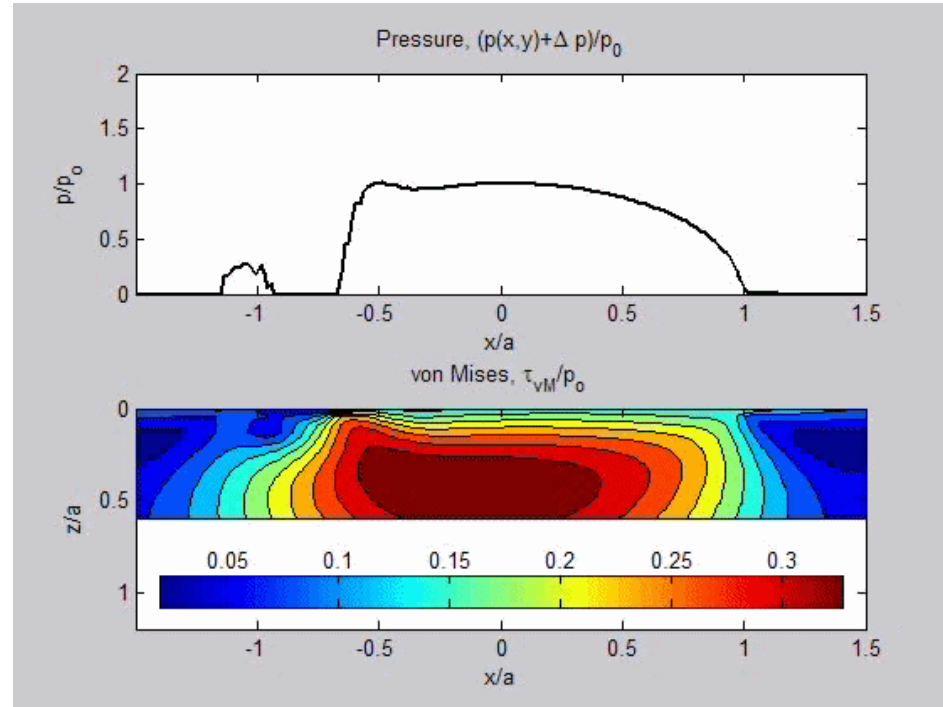
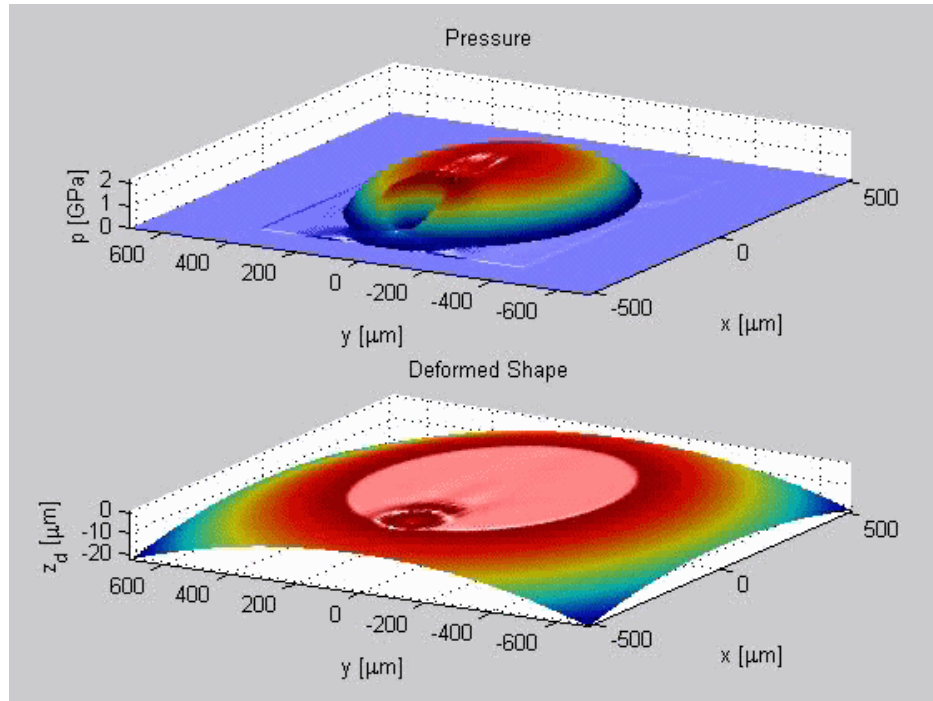
Rapid Method Pressures



(d) Pressure ripples, present scheme

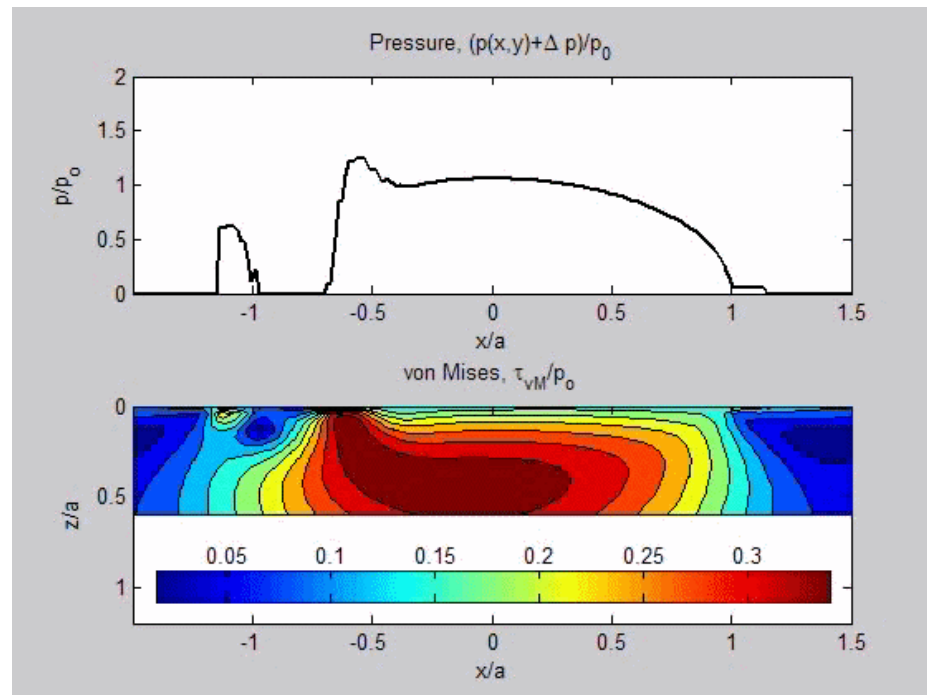
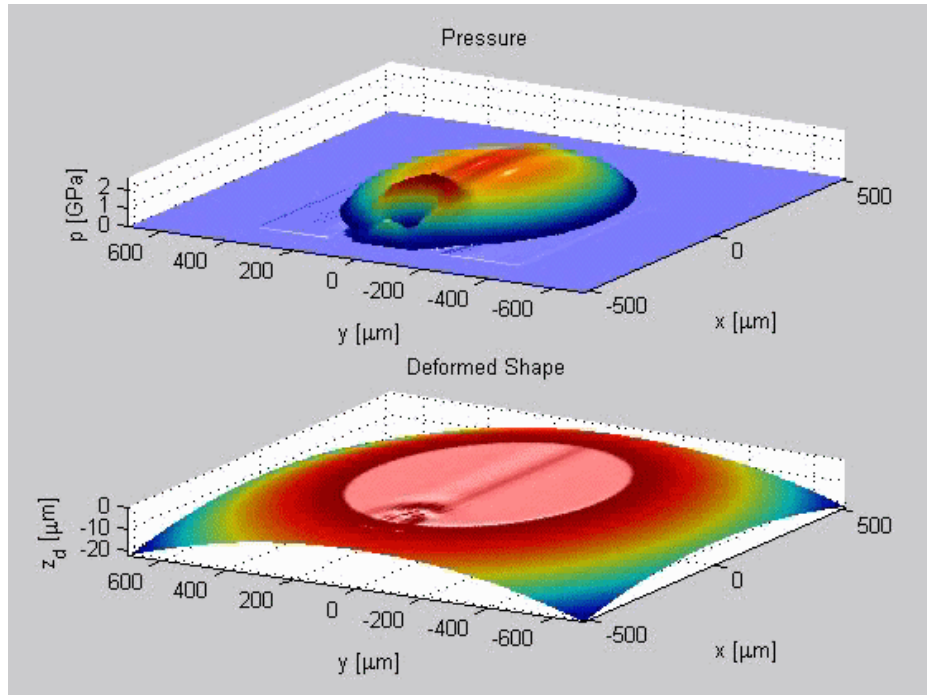
Case of Pure Rolling (Zero Sliding)

Non-Newtonian Fluid

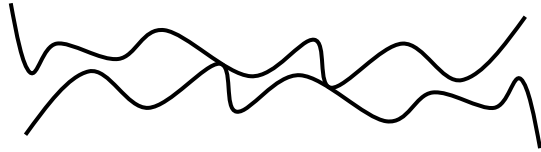


Case of Sliding, Indented Surface Moving 30% Faster

Non-Newtonian Fluid



Conversion to Mixed Lubrication



Following Stanley and Kato, assuming periodicity in roughness, in dry contact, the elastic displacements are:

$$\mathbf{u}(\mathbf{p}) = \text{IFFT} \{ \mathbf{w} \cdot \text{FFT}(\mathbf{p}) \}$$

From which the frequency response matrix is

$$w(i, j) = \frac{1}{\sqrt{(i-1)^2 + [(j-1)l]^2}},$$

$$\forall i = 1, \dots, n/2 \quad \text{and} \quad j = 1, \dots, m/2$$

$$w(i, j) = \frac{1}{\sqrt{(i-1)^2 + [(m-j+1)l]^2}},$$

$$\forall i = 1, \dots, n/2 \quad \text{and} \quad j = m/2 + 1, \dots, m$$

$$w(i, j) = \frac{1}{\sqrt{(n-i+1)^2 + [(j-1)l]^2}},$$

$$\forall i = n/2 + 1, \dots, n/2 \quad \text{and} \quad j = 1, \dots, m/2$$

$$w(i, j) = \frac{1}{\sqrt{(n-i+1)^2 + [(m-j+1)l]^2}},$$

$$\forall i = n/2 + 1, \dots, n/2 \quad \text{and} \quad j = m/2 + 1, \dots, m$$

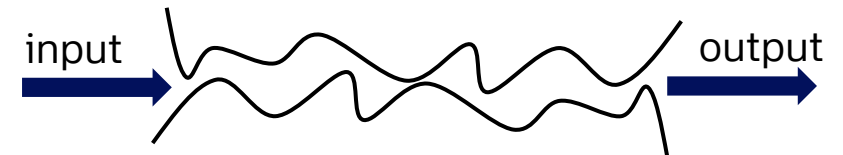
for $w(1, 1) = 0$, where $l = L_x/L_y$.

The contact problem is solved by finding p (pressures):

$$\min(f) = \frac{1}{2} \int_S p u(p) dS + \int_S p g dS$$

$$\frac{1}{A} \int_S p dS = p_{\text{target}} \quad p \geq 0$$

The mixed lubrication algorithm relies on the load sharing principle, until the flow is balanced

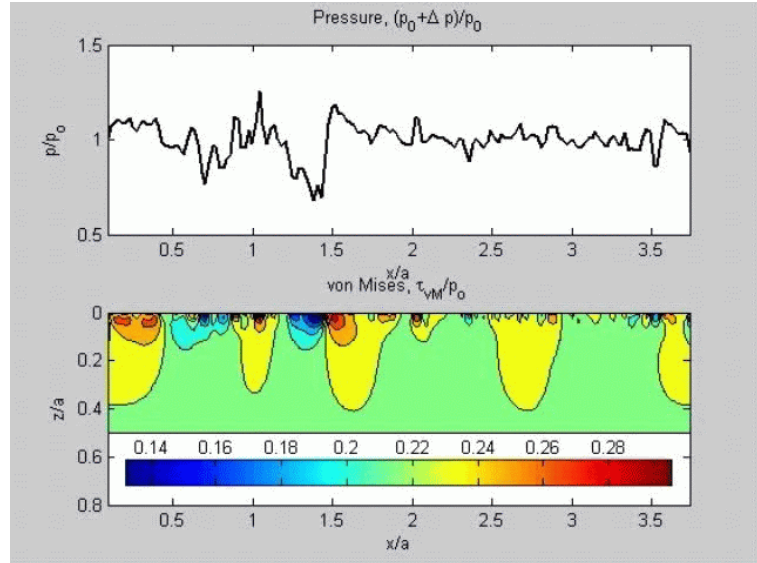
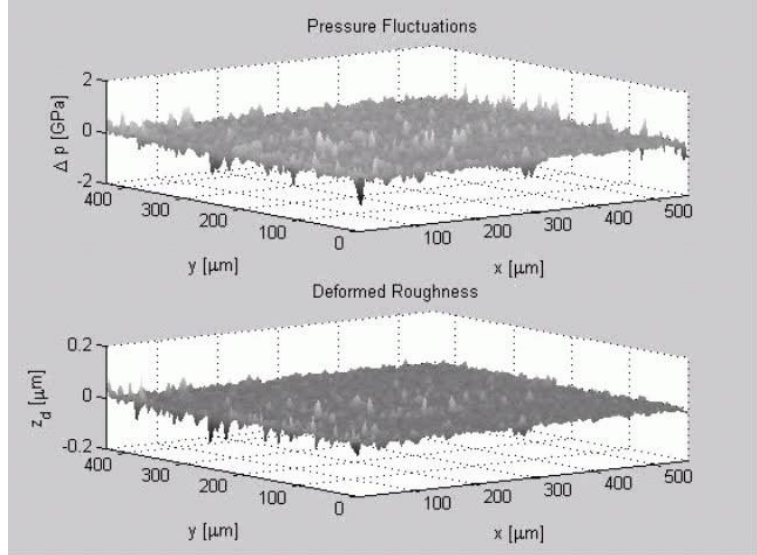
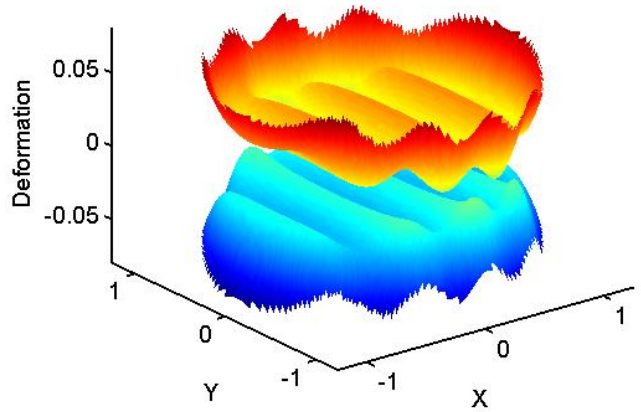
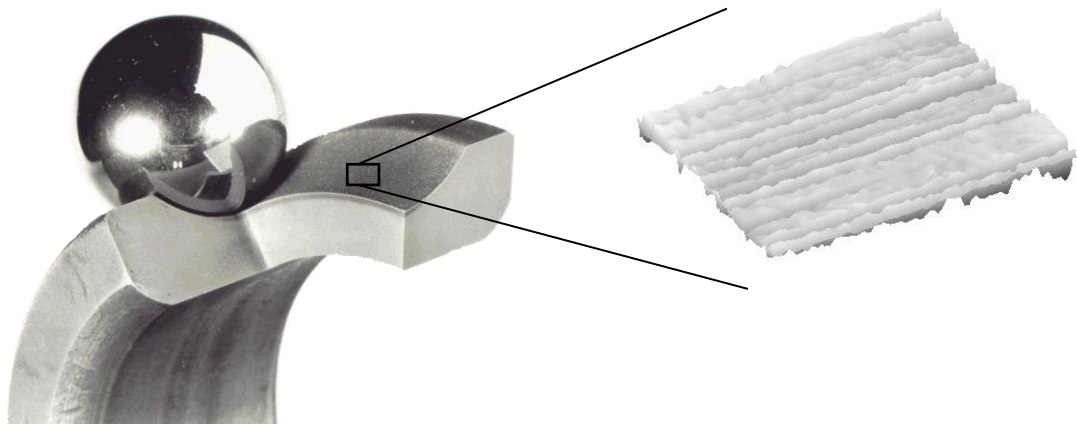


Input = output

* Morales-Espejel, G.E., Wemekamp, A.W., Félix-Quiñonez, A. Micro-geometry effects on the sliding friction transition in elastohydrodynamic lubrication IMechE, part J, J. of Eng. Trib., vol. 224, pp. 621-637, 2010

Stanley, H. M. and Kato, T. A FFT-based method for rough surface contact. *ASME, J. Tribol.*, 1997, **119**, 481-485.

Modelling Lubrication in Real Time*



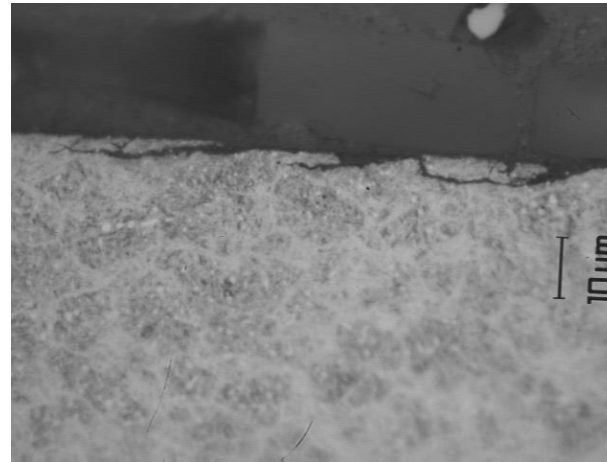
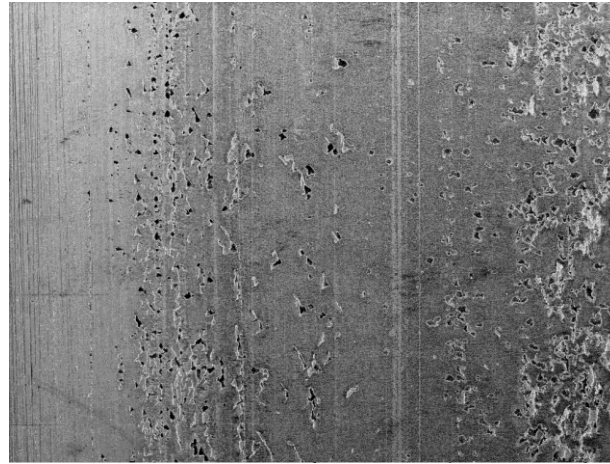
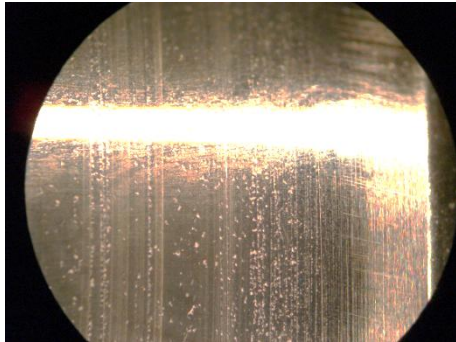
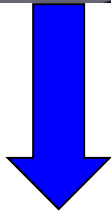
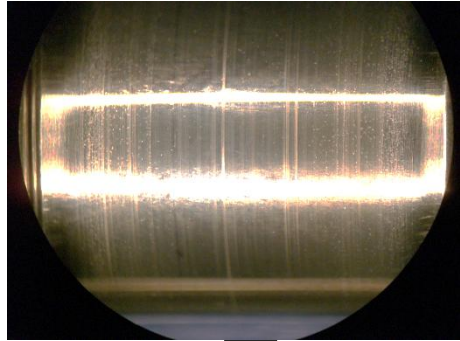
Includes:

- Roughness
- Time dependent
- Mixed-Lubrication
- Non-Newtonian
- Rolling/Sliding
- Thermal effects
- Runs as fast as the video

* Morales-Espejel, G.E., Wemekamp, A.W., Félix-Quiñonez, A. Micro-geometry effects on the sliding friction transition in elastohydrodynamic lubrication IMechE, part J, J. of Eng. Trib., vol. 224, pp. 621-637, 2010

Surface Distress

Modelling Surface Distress

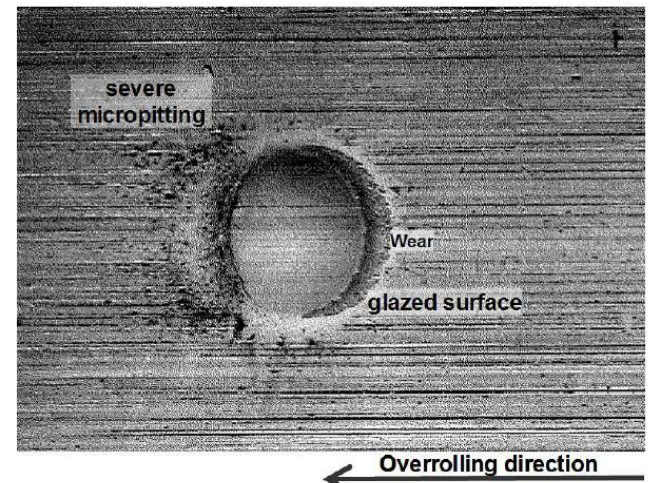
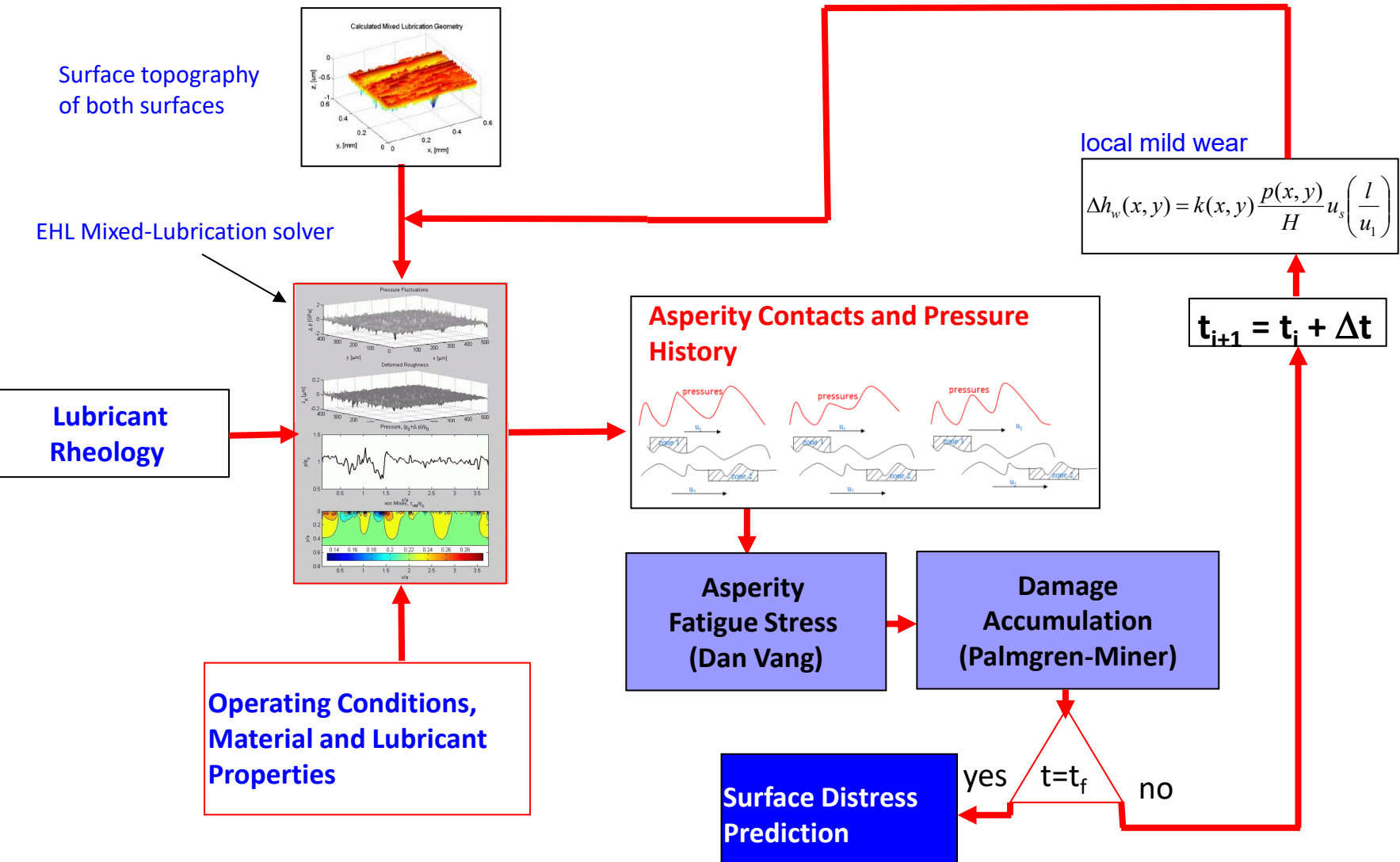


Definition Micropitting:

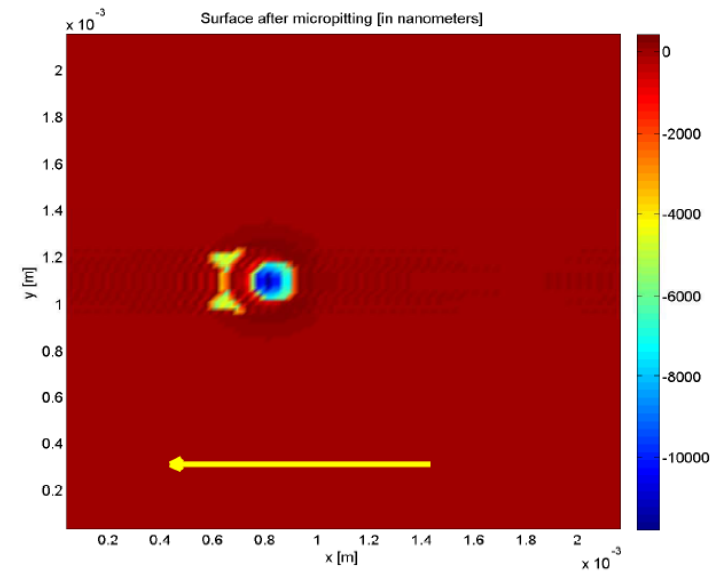
Tiny surface spalls, pits & cracks which sometimes appear on the surface of rolling-sliding contacts in poor lubrication conditions, ISO 15243 calls it surface distress

Micropitting is in fact surface fatigue at asperity level. It competes with mild wear which removes the fatigued layers of the surface.

SKF Surface Distress – Micropitting



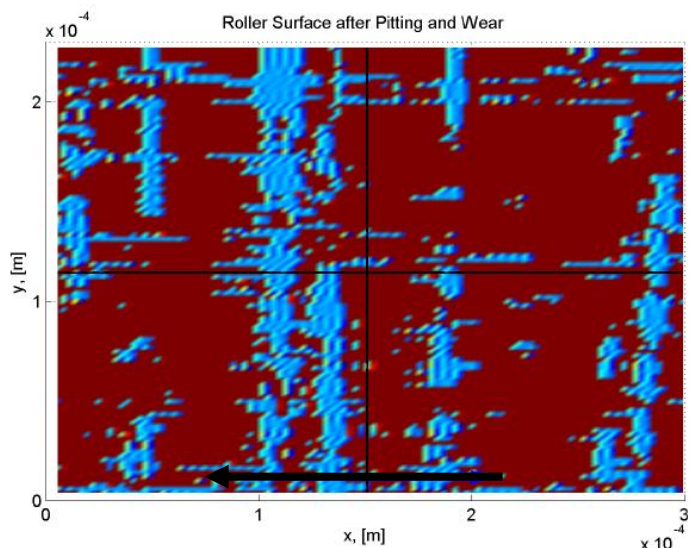
(a) Experimental 2250X10⁶ over-rollings



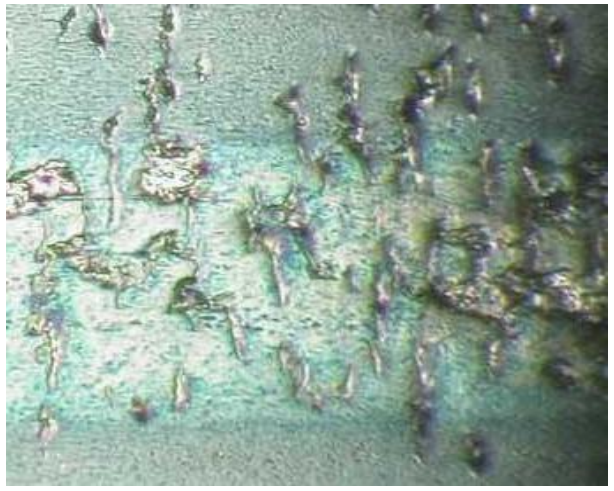
(b) Model 2250X10⁶ over-rollings

* Morales-Espejel, G.E., Brizmer, V., "Micropitting Modelling in Rolling–Sliding Contacts: Application to Rolling Bearings", Tribology Transactions, 54, pp. 625-643, 2011.

SKF Roughness Lay Effect

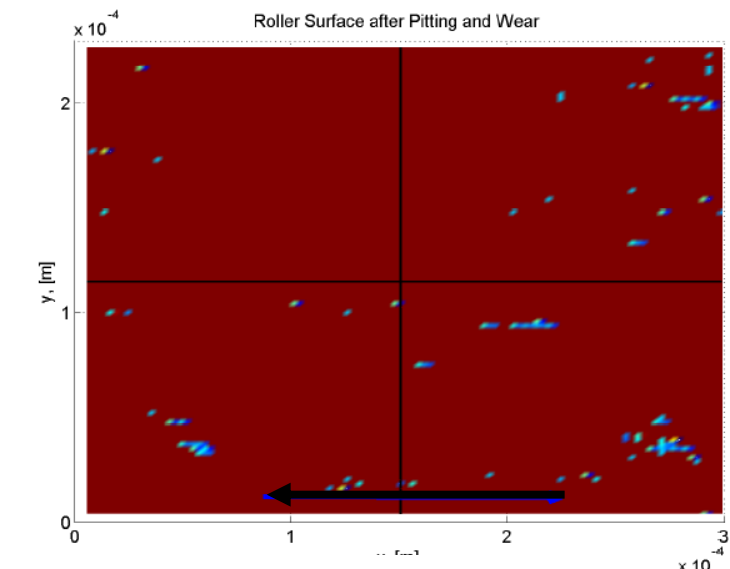
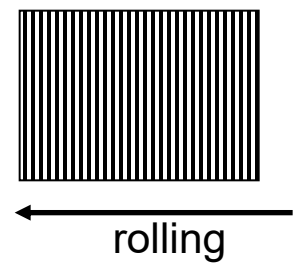


Model – Transverse Roughness



Experiment – Transverse Roughness

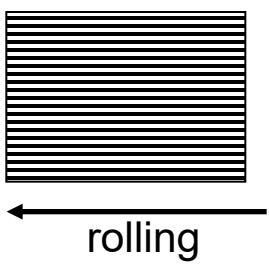
$\Lambda=0.1$
720000 cycles



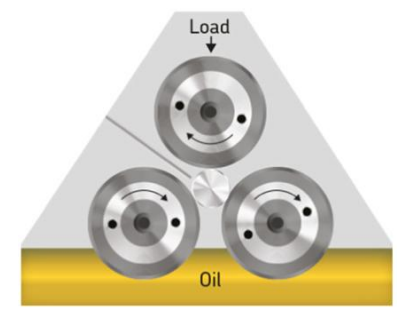
Model – Longitudinal Roughness



Experiment – Longitudinal Roughness

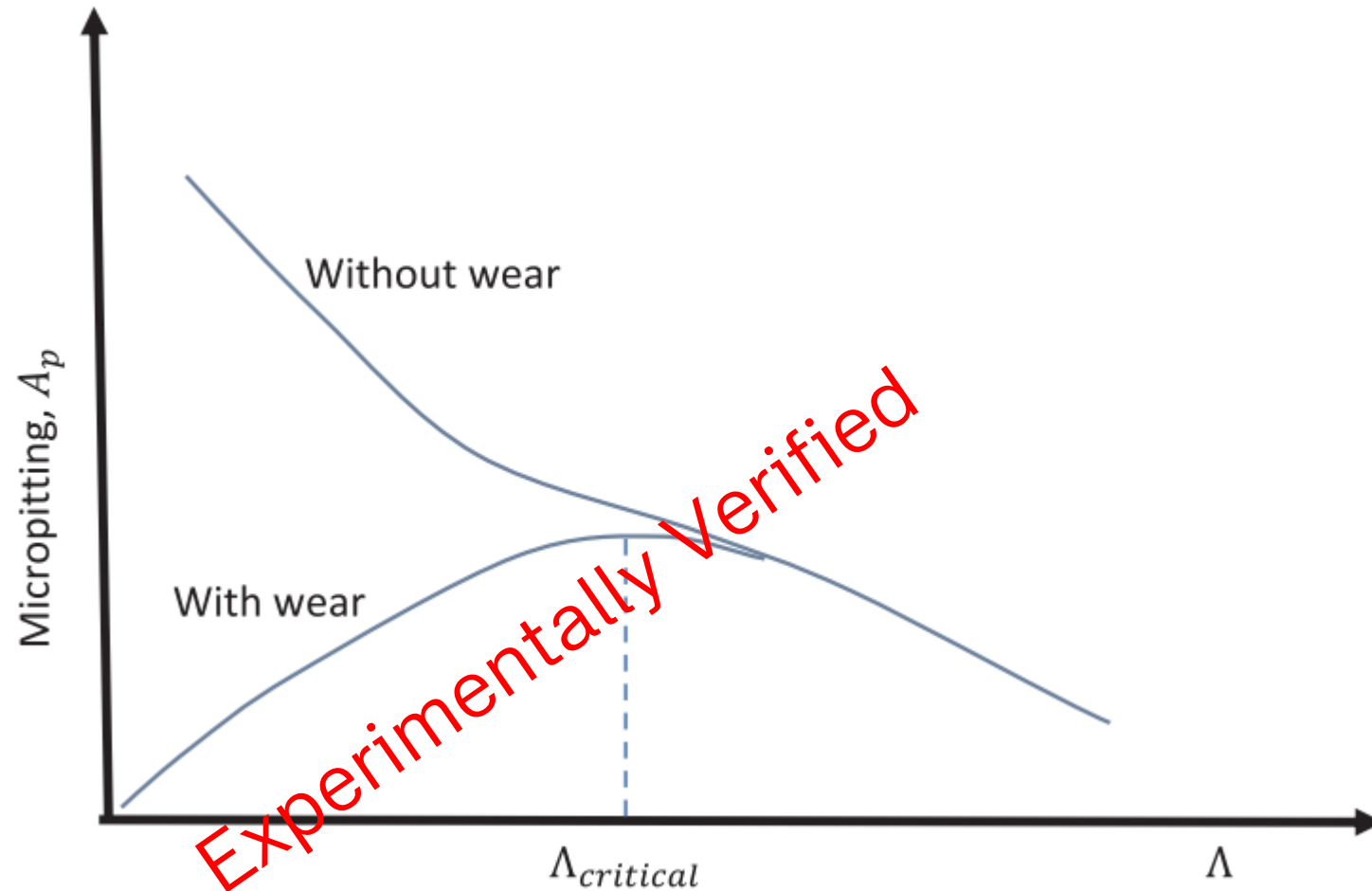


3-Disc Machine



* Morales-Espejel, G.E., Brizmer, V., "Micropitting modelling in rolling-sliding contacts: Application to rolling bearings", Trib. Trans., 54, pp. 625-643, 2011

SKF Competition with Mild Wear

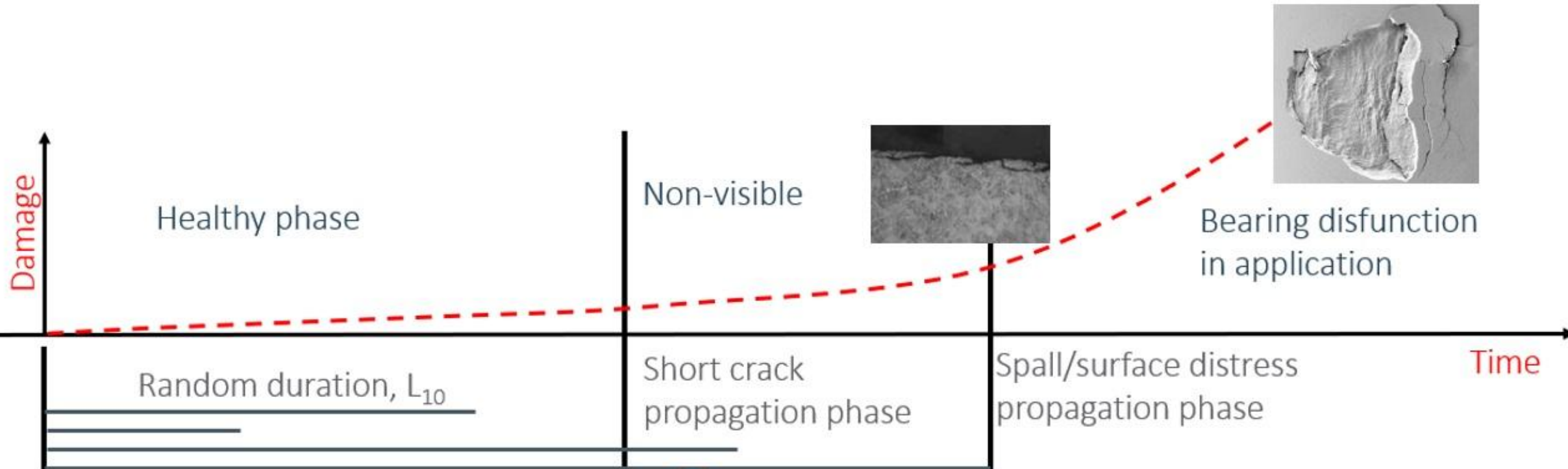


G.E. Morales-Espejel, P. Rycerz, A. Kadiric, Prediction of micropitting damage in gear teeth contacts considering the concurrent effects of surface fatigue and mild wear, in press, Wear 398–399 (2018) pp. 99–115.

New Concepts in the Life of Machine Elements

Generalized Bearing Life Model (GBLM)

The Life of Machine Elements



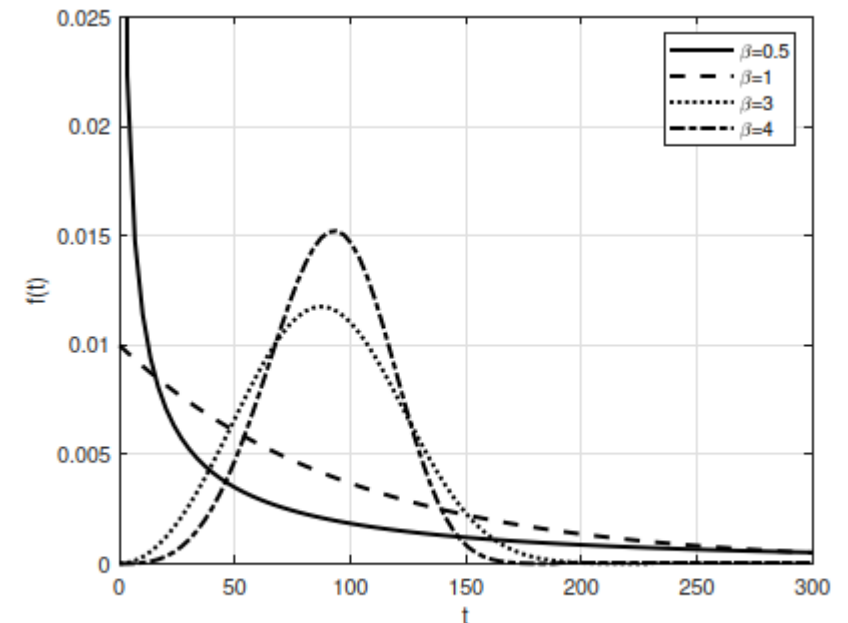
Randomness of Bearing Life

The life of rolling bearings (and other machine elements) is a random number, which follows a certain probability distribution. Therefore, it can not be calculated, it can only be estimated for a population of seemingly equal bearings running at seemingly equal operating conditions with a certain reliability (or probability of survival). Normally 90 % survival probability is used, thus the L_{10} is calculated.

Rolling Bearing Life in general follows a Weibull Probability Distribution

Weibull Density Probability Function:

$$f(t) = \frac{dF(t)}{dt} = \frac{\beta}{\tilde{\eta}} \left(\frac{t - L_0}{\tilde{\eta}} \right)^{\beta-1} \exp \left[- \left(\frac{t - L_0}{\tilde{\eta}} \right)^{\beta} \right], \forall t \geq L_0$$



(a) Density, $f(t)$

SKF Weibull Paper And Endurance Testing

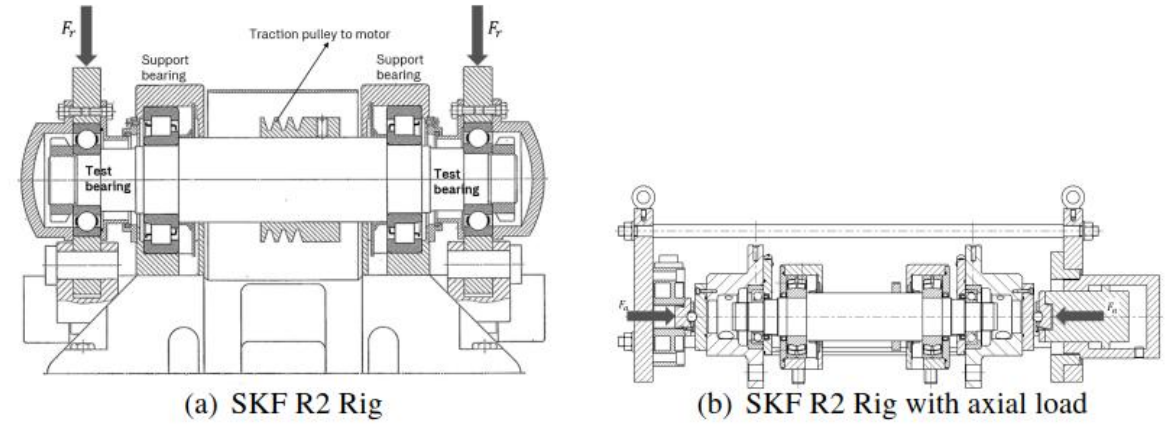
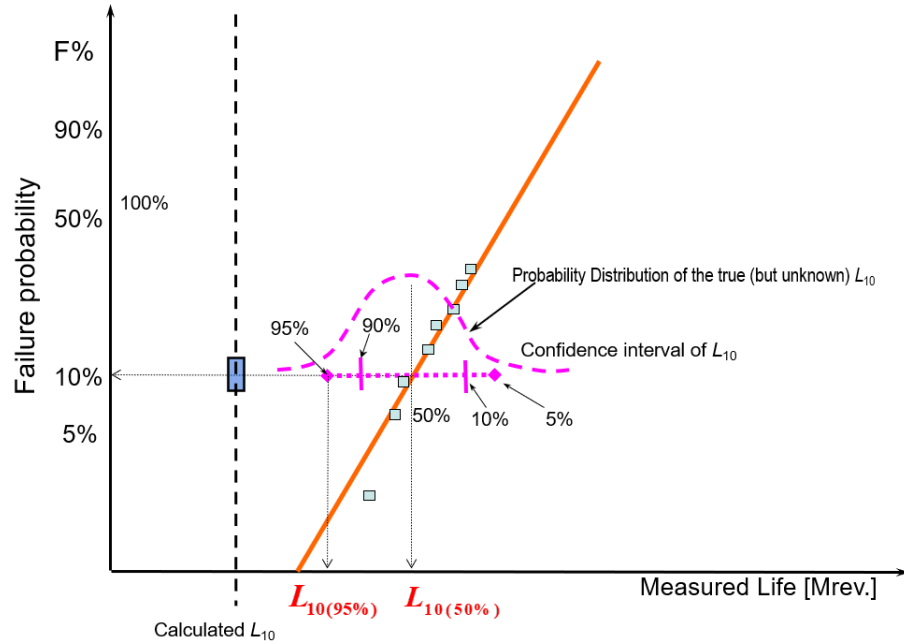


Figure 2.6 SKF R2 test rigs for small rolling bearings. (Courtesy of SKF.)

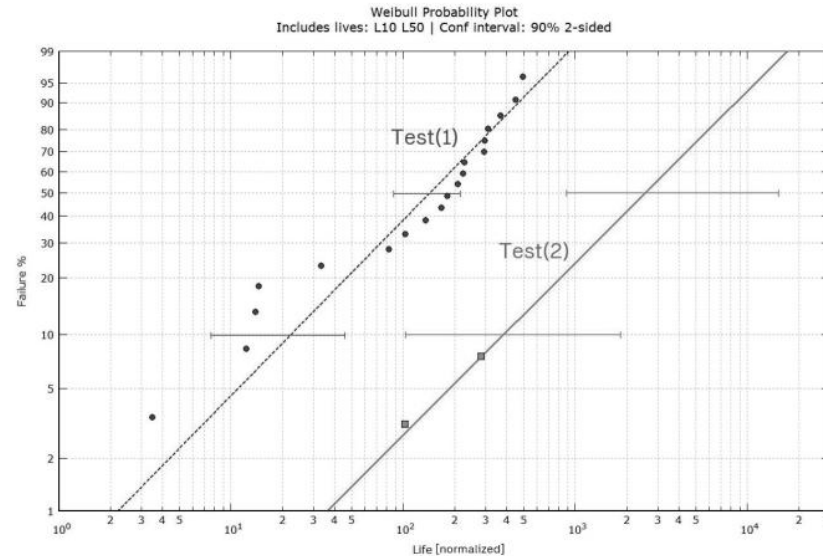
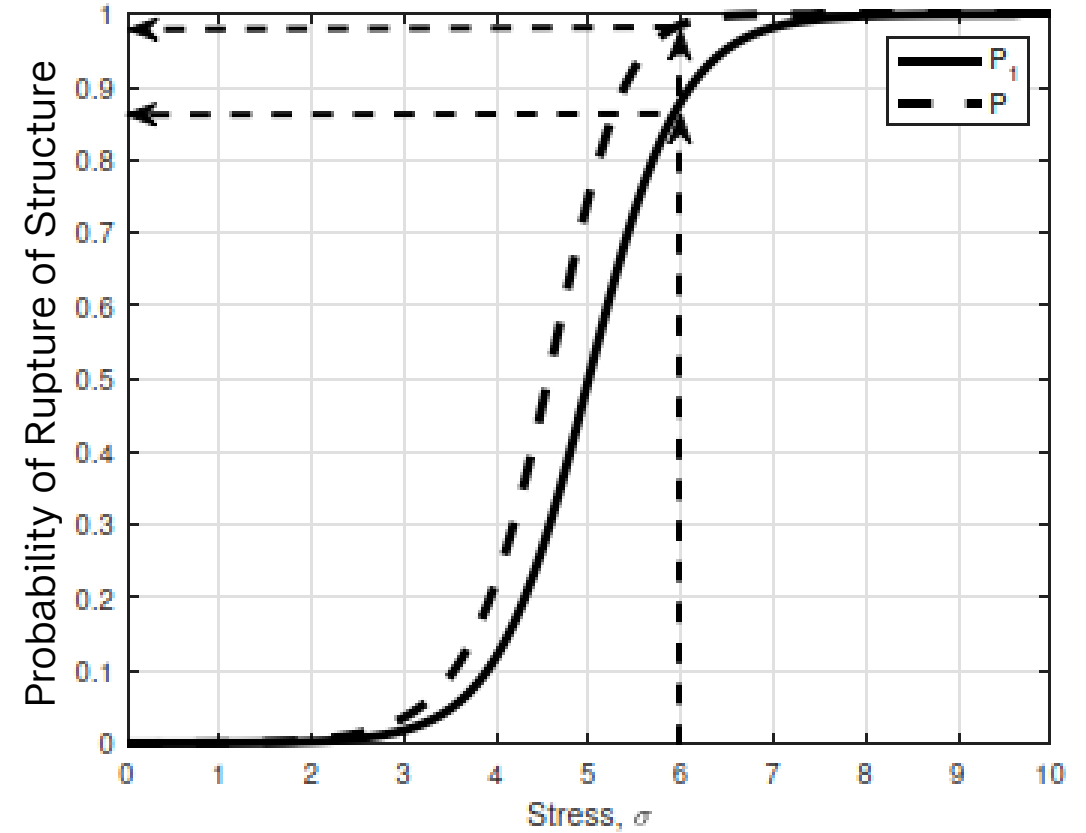
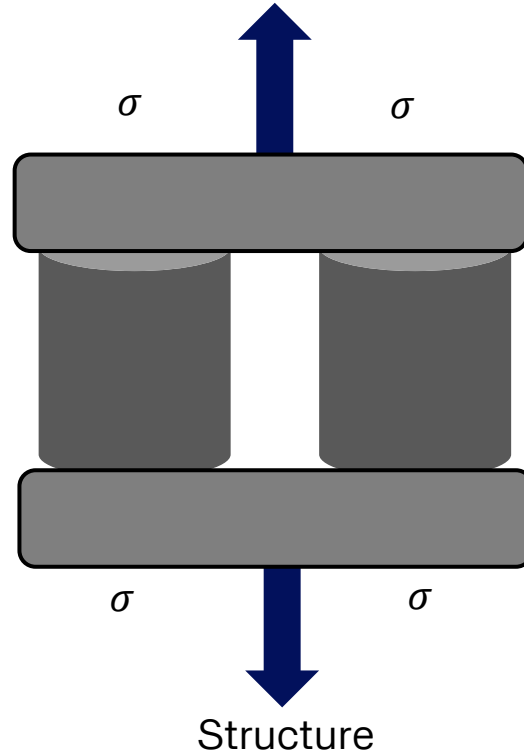
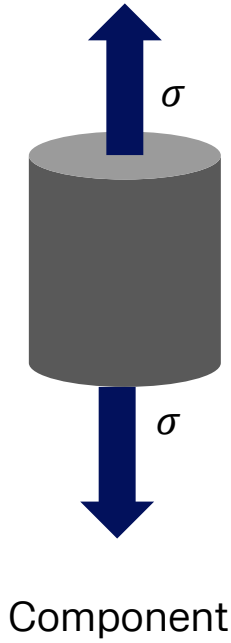


Figure 2.5 Real Weibull plot from endurance testing showing two distinct tests, including the 90% confidence intervals for L_{10} and L_{50} .

SKF Weibull Theory of Strength

Probability of rupture under stress: $P_1 = f(\sigma)$



Probability of survival under stress:

$$S = 1 - P_1$$

$$S = S_1 S_2$$
$$P = 1 - S$$

SKF Ioannides and Harris Model, Bases of current ISO 281

Starting with :

$$\ln \frac{1}{S} \propto \frac{N^e \tau_0^c V}{z_0^h} \quad \ln \frac{1}{S} = \bar{A} N^e \int_V \frac{\langle \tau - \tau_u \rangle^c}{z'^h} dV \quad z'(x, y) = \frac{\int_0^{z_{max}} (\tau - \tau_u) z dz}{\int_0^{z_{max}} (\tau - \tau_u) dz}$$

$$\langle \tau - \tau_u \rangle = \begin{cases} 0, & \forall (\tau - \tau_u) < 0 \\ (\tau - \tau_u), & \forall (\tau - \tau_u) \geq 0 \end{cases}$$

Introduction of the Fatigue Limit: τ_u

with $L = u N$, L = Life in Mrevs and N = Life in no. load cycles

Finalizing with :

$$L_{1-S} = \frac{1}{u} \left[\frac{\ln \frac{1}{S}}{\bar{A} \int_V \frac{\langle \tau - \tau_u \rangle^c}{z'^h} dV} \right]^{1/e} \xrightarrow{\text{simplification}} L_{10} = a_{SLF} \left(\frac{C}{P} \right)^p$$

E. Ioannides, G. Bergling, and A. Gabelli. An Analytical Formulation for the Life of Rolling Bearings. *Acta Polytechnica Scandinavica, Mechanical Engineering Series*, 137, pages 1–80, 2012.

Separation of Surface from Subsurface Survival

- Different failure modes can be considered
- Comparison of damage between surface and subsurface
- Differentiation of surface and subsurface design features can be highlighted
- Flexible scheme where new knowledge could be easily added

SKF Derivation: Weibull Material Strength Theory

A STATISTICAL THEORY OF THE STRENGTH OF MATERIALS

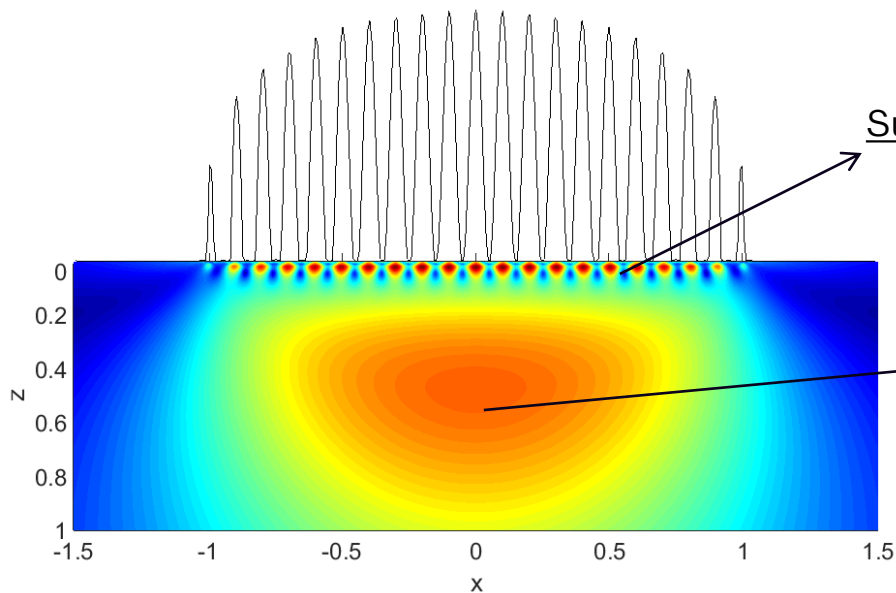
BY

W. WEIBULL

Professor, Royal Technical University, Stockholm



A pseudo- Hertzian Contact



Surface: Tribology models

Sub-Surface: Hertzian Rolling Contact Fatigue

that the probability of rupture of each rod is S The probability of each rod withstanding the load is $S_i = 1 - S$. According to the theory of probability, the probability S_{12} that two events having the probabilities

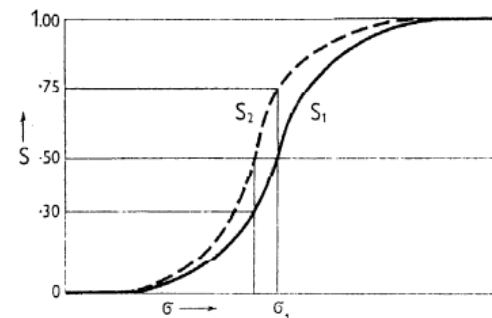


Fig. 1.

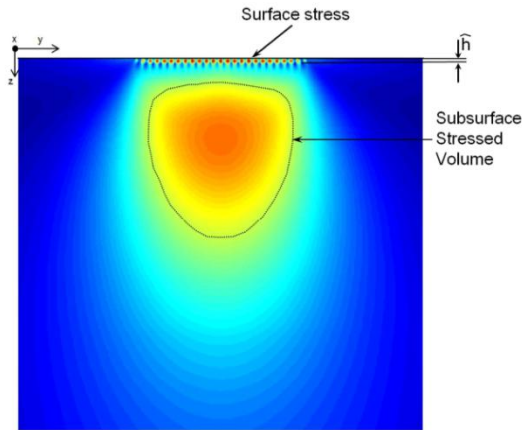
S_1 and S_2 respectively occur simultaneously is obtained by multiplying the two individual probabilities, or

$$S_{12} = S_1 \cdot S_2 \dots \dots \dots 1)$$

which may, of course, also be expressed in the equivalent form

$$\log S_{12} = \log S_1 + \log S_2 \dots \dots \dots 2)$$

Generalized Bearing Life Model (GBLM)



The probability of survival for different regions:

$$S_1^n = S_1 \cdot S_2 \cdots S_n = \prod_{i=1}^n S_i$$

$$\ln \left[\frac{1}{S(N)} \right] = \ln \left[\frac{1}{\Delta S_1(N)} \right] + \ln \left[\frac{1}{\Delta S_2(N)} \right] + \cdots + \ln \left[\frac{1}{\Delta S_n(N)} \right]$$

Introducing the material degradation functions $G_{v,n}$:

$$\ln \left[\frac{1}{S(N)} \right] = \int_{V_{v,1}} G_{v,1}(N) dV_{v,1} + \int_{V_{v,2}} G_{v,2}(N) dV_{v,2} + \cdots + \int_{V_{v,n}} G_{v,n}(N) dV_{v,n}$$

Reducing only to Subsurface (V) and Surface (A):

$$\ln \left[\frac{1}{S(N)} \right] = \int_{V_v} G_v(N) dV_v + \hat{h} \int_A G_s(N) dA$$

GBLM

For the volume (as before) G_v :

$$G_v = \bar{A} N^e \frac{\langle \sigma - \sigma_u \rangle^c}{z^h}$$

For the area G_s :

$$G_s = \bar{B} N^e \langle \sigma - \sigma_u \rangle^c$$

Substituting back in the integrals:

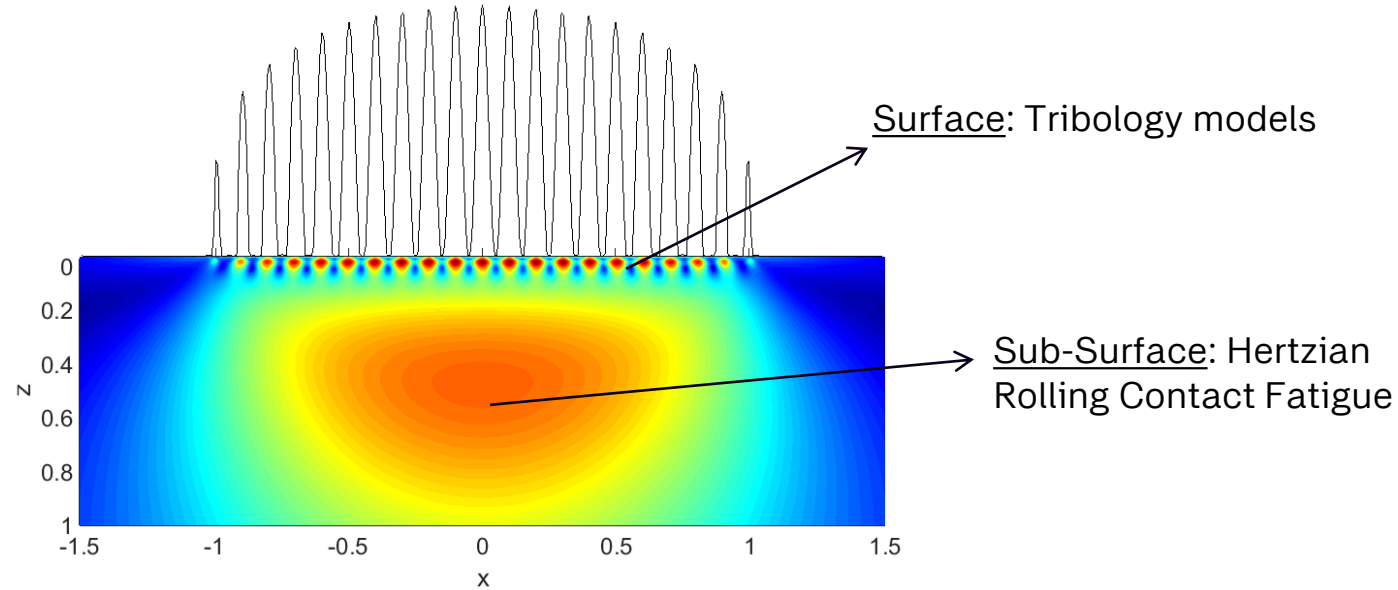
For the volume (as before) G_v :

with $L = u N$, L = Life in Mrevs and N = Life in no. load cycles

Solving for L_{1-S} :

$$L_{1-S}^e = \frac{\ln\left(\frac{1}{S}\right)}{u^e \left[\bar{A} \int_{V_v} \frac{\langle \sigma_v - \sigma_{u,v} \rangle^c}{z^h} dV_v + (uL)^{(m-e)} \bar{B} \int_A \langle \sigma_s - \sigma_{u,s} \rangle^c dA \right]}$$

SKF Generalized Bearing/Gear Life Model



$$L_{10} = \frac{\left[\ln \left(\frac{1}{0.9} \right) \right]^{1/e}}{u} \left[\bar{A} \int_{V_v} \frac{\langle \sigma_v - \sigma_{u.v} \rangle^c}{z^h} dV_v + \bar{B} \int_A \langle \sigma_s - \sigma_{u.s} \rangle^c dA \right]^{-1/e}$$

subsurface

surface



Tribology Transactions, 58: 894–906, 2015
 Published with license by Taylor & Francis
 ISSN: 1040-2004 print / 1547-397X online
 DOI: 10.1080/10402004.2015.1025932

stle
 Society of Tribologists
 and Lubrication Engineers

A Model for Rolling Bearing Life with Surface and Subsurface Survival—Tribological Effects

GUILLERMO E. MORALES-ESPEJEL,^{1,2} ANTONIO GABELLI,¹ and ALEXANDER J. C. DE VRIES¹

¹SKF Engineering & Research Centre, Nieuwegein, The Netherlands

²Université de Lyon, INSA-Lyon, CNRS, LaMCoS UMR5259, F69621, France

TRIBOLOGY TODAY, Istanbul Turkey, 13-17 April 2026

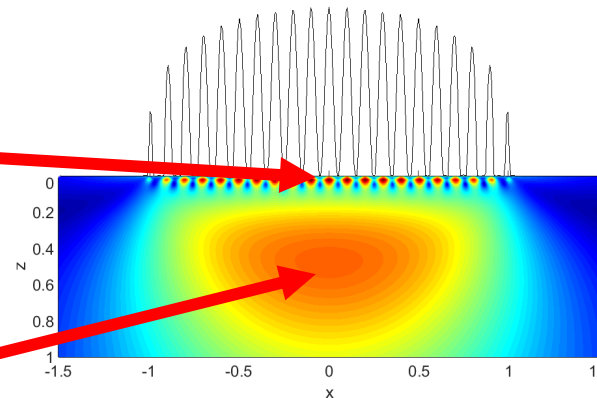
Relative Surface Fatigue Index

$$L_{10} = \frac{\left[\ln\left(\frac{1}{0.9}\right) \right]^{1/e}}{u} \left[\bar{A} \int_{V_v} \frac{\langle \sigma_v - \sigma_{u.v} \rangle^c}{z^h} dV_v + \bar{B} \int_A \langle \sigma_s - \sigma_{u.s} \rangle^c dA \right]^{-1/e}$$

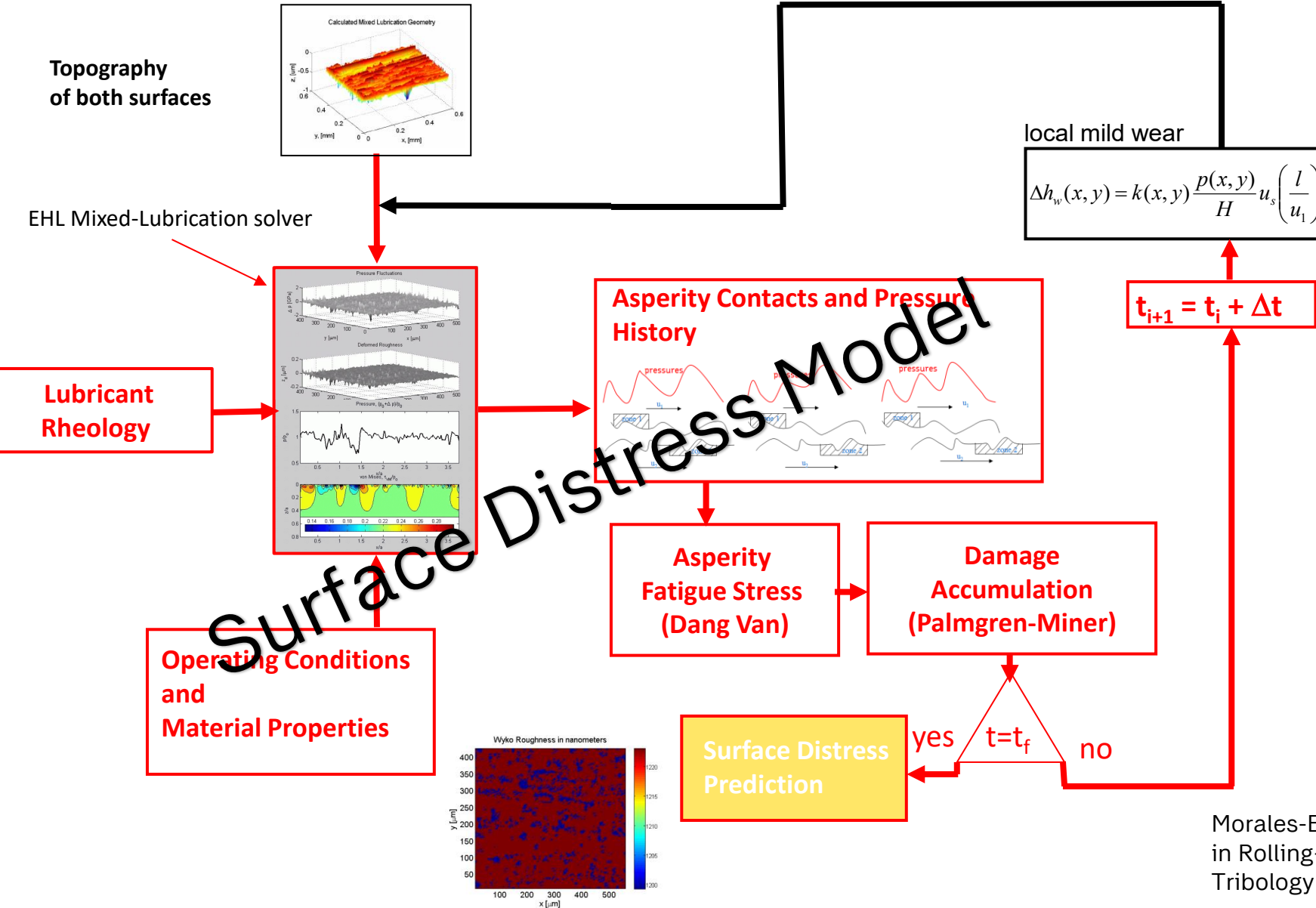
$$I_{SS} = \bar{A} \int_{V_v} \frac{\langle \sigma_v - \sigma_{u.v} \rangle^c}{z^h} dV_v$$

$$I_S = \bar{B} \int_A \langle \sigma_s - \sigma_{u.s} \rangle^c dA$$

$$S_R = \frac{I_S}{I_S + I_{SS}} \left\{ \begin{array}{l} 1 \\ 0 \end{array} \right.$$



SKF Application to Surface Fatigue



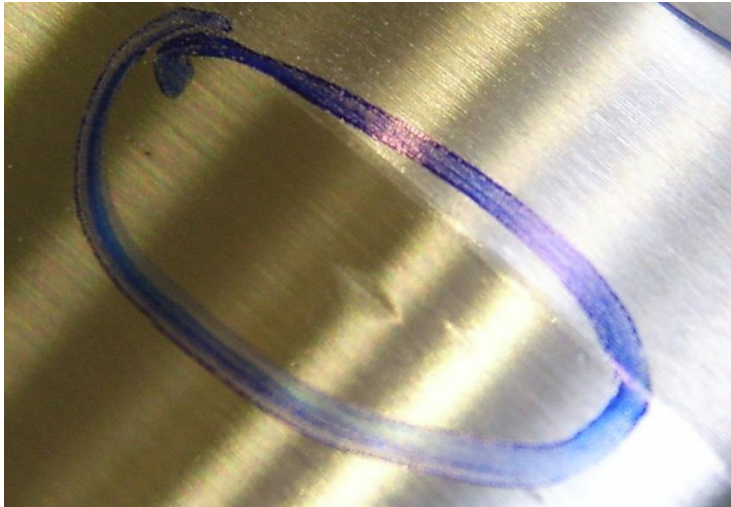
Using the advanced surface distress model It is possible to curve fit:

$$I_S = \int_A \langle \sigma_s - \sigma_{u.s} \rangle^c dA$$

$$R_s = u^m I_s \approx f_1 \exp \left[\frac{f_2}{(P/P_u)^{f_3}} + \frac{f_4}{(P/P_u)^{f_5}} + \frac{f_6}{(P/P_u)^{f_7}} \right]$$

Morales-Espejel, G.E., Brizmer, V., "Micropitting Modelling in Rolling-Sliding Contacts: Application to Rolling Bearings", Tribology Transactions, 54(4), pp 625-643, 2011.

SKF Indentation Damage

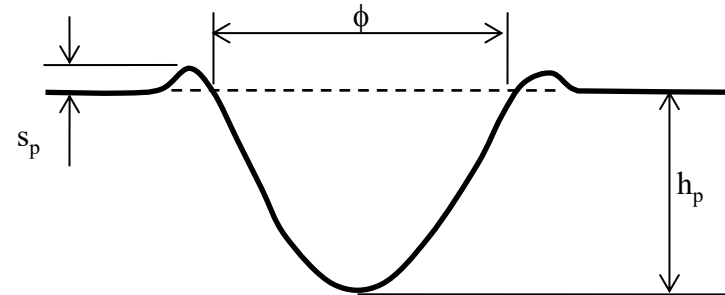


Keep a volume integral at the Surface:

$$L_{10} = \frac{\left[\ln\left(\frac{1}{0.9}\right) \right]^{1/e}}{u} \left[\bar{A} \int_{V_v} \frac{\langle \sigma_v - \sigma_{u.v} \rangle^c}{z^h} dV_v + \bar{B} \int_A \langle \sigma_s - \sigma_{u.s} \rangle^c dA + \bar{C} \sum_{i=1}^n \int_{V_v} \frac{\langle \sigma_s - \sigma_{u.s} \rangle^c}{z^h} dV_v \right]^{-1/e}$$

subsurface
surface
indentations

Idealised indentation shape:

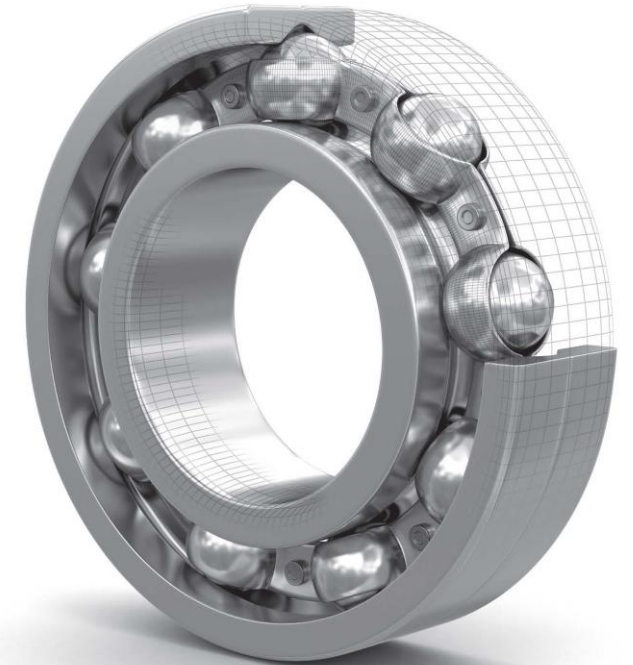


Conclusions

- Understanding Tribology is crucial to model modern machine component life.
- Deterministic models are being developed for other failure modes than just subsurface fatigue and they can be incorporated in L10 models.
- Deterministic models for failure modes must consider the competition of the different damaging mechanisms to properly capture a realistic behaviour.

ROLLING BEARINGS

Tribology Damage Modes
and Life Modelling



GUILLERMO E. MORALES-ESPEJEL

